



**VERIFICATION OF EINSTEIN GENERAL
THEORY OF RELATIVITY WITH
GRAVITATIONAL WAVES**

By

Abel Habtie Alemu

**A THESIS SUBMITTED TO
GRADUATE PROGRAMS OF
ADDIS ABABA UNIVERSITY
IN PARTIAL FULFILLMENT FOR THE REQUIREMENTS
OF THE DEGREE
MASTER OF SCIENCE IN PHYSICS
(ASTRONOMY/ASTROPHYSICS)
ADDIS ABABA, ETHIOPIA
JULY 2021**

ADDIS ABABA UNIVERSITY
PROGRAM OF GRADUATE STUDIES

VERIFICATION OF EINSTEIN GENERAL THEORY OF
RELATIVITY WITH GRAVITATIONAL WAVES

By
Abel Habtie Alemu
Department of Physics
Addis Ababa University

Approved by the Examining Board:

Dr. Remudin Reshid
Advisor

Signature

Dr. Teshome Senbeta
Examiner

Signature

Dr. Tilahun Tesfaye
Examiner

Signature

Date: July 2021

ADDIS ABABA UNIVERSITY

Date: **July 2021**

Author: **Abel Habtie Alemu**

Title: **Verification of Einstein General Theory of
Relativity with Gravitational Waves**

Department: **Department of Physics**

Degree: **M.Sc.** Convocation: **April** Year: **2021**

Permission is herewith granted to Addis Ababa University to circulate and to have copied for non-commercial purposes, at its discretion, the above title upon the request of individuals or institutions.

Signature of Author

THE AUTHOR RESERVES OTHER PUBLICATION RIGHTS, AND NEITHER THE THESIS NOR EXTENSIVE EXTRACTS FROM IT MAY BE PRINTED OR OTHERWISE REPRODUCED WITHOUT THE AUTHOR'S WRITTEN PERMISSION.

THE AUTHOR ATTESTS THAT PERMISSION HAS BEEN OBTAINED FOR THE USE OF ANY COPYRIGHTED MATERIAL APPEARING IN THIS THESIS (OTHER THAN BRIEF EXCERPTS REQUIRING ONLY PROPER ACKNOWLEDGEMENT IN SCHOLARLY WRITING) AND THAT ALL SUCH USE IS CLEARLY ACKNOWLEDGED.

This Work is Dedicated

to

*My brothers Mulugeta Asfie and Kalamlak Azanaw died
in 1995 / 1997E.C*

Table of Contents

Table of Contents	v
List of Table	viii
List of Figures	ix
Acknowledgements	xii
Abbreviations	xiii
Physical Constants	xiv
Symbols	xv
Abstract	xvi
1 Introduction	1
1.1 Objective of the thesis	4
1.1.1 General objective	4
1.1.2 Specific objectives	4
1.2 Thesis outline	4
2 General theory of relativity and gravitational waves	5
2.1 Introduction	5
2.2 General theory of relativity	5
2.2.1 Equivalence principle	5
2.2.2 Special theory of relativity	6
2.2.3 Prediction of general relativity	9
2.3 Direct and generic tests of general relativity	10
2.3.1 Direct test	10
2.3.2 Generic tests	10
2.4 Gravitational waves	10

2.5	Sources of gravitational waves	11
2.5.1	Compact binary coalescence	11
2.5.2	Continuous wave sources	16
2.5.3	Burst sources	17
2.5.4	Stochastic background	19
2.6	Gravitational radiation as a tool for testing general relativity	20
2.6.1	Tests of scalar-tensor gravity	20
2.6.2	GR from in-spiral-merger-ring down consistency test	22
2.7	Properties of gravitational waves	23
2.7.1	Polarization of gravitational waves	24
2.7.2	Speed of gravitational waves	25
2.8	The use of gravitational waves to test general relativity	26
2.9	Gravitational waves detection	27
2.10	Summary	32
3	Methods of analyzing gravitational waves to verify Einstein general theory of relativity in binary black hole and its waveform models	33
3.1	Introduction	33
3.2	Einstein field equation	33
3.2.1	Einstein equations in empty space	36
3.2.2	Linear approximation of Einstein field equations	37
3.2.3	Quadrupole formalism	38
3.2.4	Two-body problem	39
3.3	Numerical relativity	41
3.4	Effective one body formalism	43
3.5	IMRPhenom	44
3.6	Summary	44
4	Result And Discussion	45
4.1	Introduction	45
4.1.1	Plus and cross polarization of gravitational waves	45
4.1.2	Power spectral density	46
4.1.3	Signal to noise ratio	47
4.1.4	Change of the waveform with the mass of the binary	49
4.1.5	Change of the waveform with distance from the source of the binary	50
4.1.6	Waveform comparison	51

4.2 Summary	52
5 Conclusion	53
Bibliography	54

List of Tables

2.1	Potentially achievable bounds on λ_g from gravitational-wave observations of in-spiraling compact binaries [25].	26
-----	--	----

List of Figures

2.1	The causal structure of spacetime [10]	7
2.2	The curvature of space-time caused by the sun and the earth, represented by a grid. The spacetime around the Sun is warped due to its mass. The Earth then merely follows a geodesic, or a locally straight path, in this curved spacetime. However, since the spacetime itself is curved, this locally straight path becomes a curved path on a global scale; an ellipse in this instance. The Earth also warps the spacetime around itself, which causes the Moon to orbit it [14].	8
2.3	Orbits of binary system around their comen center of masses [17]. . .	12
2.4	Coalescence of binary black holes. The loss of energy and angular momentum via the emission of gravitational radiation drives compact-binary coalescence, which proceeds in three different phases. The strongest gravitational-wave signal, illustrated here because the gravitational-wave amplitude h , accompanies the late in-spiral phase and therefore the plunge and merger phase; for that a part of the coalescence, post-Newtonian and perturbation methods break down, and numerical simulations must be used [23].	16
2.5	Comparison of different stochastic gravitational wave background measurements and models [2].	20
2.6	The right panel describe Posterior distributions for the parameters $\Delta M_f/M_f$ and $\Delta a_f/a_f$ that describe the fractional difference in the estimates of the final mass and spin from in-spiral and post-in-spiral signals. The contour shows the 90% confidence region. The plus symbol indicates the expected GR value (0, 0) [28]. There is a significant overlap. (Image credit: LIGO)	23

2.7	The gravitational waveform in this figure correspond to the primary detection event GW150914. The gravitational wave strain is plotted against the clock. the top two panels show the detector output from the LIGO Hanford and LIGO Livingston. The waveform predicted from general theory of relativity are superimposed on the detector output. the underside panel shows the detector output from the LIGO Livingston detector together with that from LIGO Hanford detector shifted appropriately taking under consideration the suspension within the arrival of signal and therefore the difference within the detector orientations. They match well indicating that the identical signal was detected in both the detectors (Image credit: LIGO) [13]. .	30
3.1	Two bodies with equal masses orbiting around their center of mass in circular orbits [11].	40
3.2	Numerical waveform template.	42
4.1	Waveform for the IMRPhenomB model of both polarization after inverse Fourier transform, the figure constructed from two equal $20M_{\odot}$ of black hole with lower frequency of $40Hz$, the right one is zoomed around the time of the merger. We have a better view on the ring down part, where the amplitude decreases to zero. A shift can be observed between the two polarization.	46
4.2	zoomed and whitening data over the range of 20 Hz to 400 Hz around the event time = 1126259462.422 se. The left panel shows the Hanford data and the right panel shows the Livingston data at the time of GW150914.	47
4.3	SNR with the detectable duration of time in second(s). The two figure is detected from LIGO Hanford (pink) and LIGO Livingston(green). The two-wave signals are the same but the amplitude of the wave detected at Hanford detector is longer than the wave detected from Livingston detector and these are similar to the gravitational wave predicted from the merger of the binary black hole or binary neutron stars.	48

4.4	Gravitational wave signal for different mass of binary system for the IMRPhenomB model. We see that the amplitude, as well as the frequency are modified, from the in-spiral to the ring-down phase. The left panel constructed from two equal masses of black holes the amplitude of wave is small compared to the right one. The right panel one mass of the black hole kept fixed($10 M_{\odot}$) whereas the second masses free to change.	49
4.5	Gravitational wave amplitude detecting at different distance from the Earth and variation of waveform models SEOBNRv4(left panel) and IMRPhenomA(right panel).	50
4.6	Time domain waveform SEOBNR stands for Spin Effective One Body Numerical Relativity, this model is calibrated to a set of numerical relativity simulations and frequency domain IMRPhenom, stands for phenomenological In-spiral-Merger-Ring down model, the models of the waveform by phenomenological predicting the amplitude and phase evolution. This waveform family is also calibrated to a set of numerical relativity simulations.	51
4.7	waveform comparison between NR, SEOBNRv2 and IMRPhenomB wave models.	52

Acknowledgements

First of all, I thanks to God for His unlimited love, care, and undesirable help He has done to me throughout my life. I would like to express my deep gratitude to my advisor and instructor Dr. Remudin Reshid for his continuous guidance and great support. I would like to extend my thanks to my instructors and the department of physics of the Addis Ababa University and its staffs, I have learned many things from them like respecting teaching profession, punctuality, encouraging learners to have creative mind and so on. I would also like to acknowledge the financial support for my studies provided by the Addis Ababa Educational Bureau. Finally, I am very grateful thanks to my friends Murad Yimam, Debela Alemayehu, Jemal Regassa, Natnael and all my classmates I have received many comments and feed backs.

Addis Ababa University

Abel Habtie Alemu

April, 2021

Abbreviations

ASD	Amplitude Spectral Density
AXPs	Anomalous X-Ray Pulsars
EFE	Einstein Field Equation
BBH	Binary Black hole
BBN	Big Bang Nucleosynthesis
BHNS	Black hole Neutron Star
CBC	Compact Binary Coalescence
CMBR	Cosmic Microwave Background Radiation
CW	Continuous Wave
PN	Post Newtonian
GRBs	Gama-ray Bursts
GR	General Relativity
GW	Gravitational Wave
LIGO	Laser Interferometer Gravitational Wave Observatory
LISA	Laser Interferometer Space Astronomy
MBH	Massive Black hole
NR	Numerical Relativity
SEOBNR	Spin Effective One Body Numerical Relativity
IMRPhenom	In-spiral Merge Ringdown Phenomenological
PSDs	Power Spectral Density
SGRS	Soft Gama-ray Repeaters
SNR	Signal to Noise Ratio

Physical Constants

Speed of Light	$C = 2.99792458 \times 10^8 \text{ ms}^{-2}$
Universal Gravitational Constant	$G = 6.67 \times 10^{-11} \text{ Nm}^2 \text{ kg}^{-2}$
Mega parsec	$\text{Mpc} = 3.08568025 \times 10^{24} \text{ cm}$
Planck luminosity	$L_0 = 10^{59} \text{ egr/s}$
Mass of the Sun	$M_{\odot} = 1.99 \times 10^{33} \text{ g}$
Kilo parsec	$\text{kpc} = 3.08568025 \times 10^{21} \text{ cm}$
luminosity of the Sun	$L_{\odot} = 3.839 \times 10^{33} \text{ erg/s}$
Positive Cosmological constant	$\Lambda = (10^{16} \text{ ly})^{-2}$
Hubble's constant	$H_0 = 70.65 \text{ km/s/Mpc}$

Symbols

f_{GW}	Gravitational Wave frequency in Hz
L	Total radiated luminosity in erg/s
τ	Time remaining before coalescence in second(s)
M_c	Chirp mass in M_\odot
ρ_{crit}	Critical energy density in eV/cm^3
D_l	Luminosity distance of the from the source to Earth in Mpc
S_{GW}	Power spectral density in unit of egr/sHz

Abstract

Gravitational wave science is one of direct observation of the waves predicted by Einstein's general theory of relativity and opening the exciting new field of gravitational wave astronomy. In this thesis work we study gravitational waves and we also present some of the general relativity test of gravitational wave such as linear approximation of Einstein field equation which is Einstein equation for a weak gravitational field simply $\square h_{\mu\nu} = 0$, thus, the metric perturbations satisfy the flat space wave equation and the solutions can therefore be interpreted as gravitational waves polarization (plus and cross polarization). In this thesis We also found that gravitational wave emits when BBHs are spiraling with each other. We suggested that high amplitude of gravitational waves are formed around merger of BBHs, the amplitude of GWs large for high masses and also the amplitude falls when the waves moves away from the source like standard siren's of $h \propto \frac{1}{r}$. We also checked that SEOBNR and IMRPhenom models are matched with prediction of GR simulated by NR and the waveform observed from LIGO. These waveform comparison tells us Einstein general theory of relativity passes the test of GW.

Introduction

Gravity governs the structure and evolution of the whole Universe, and it's successfully described by Einstein's general theory of relativity. General theory of relativity is the geometric theory of gravity published by Albert Einstein in 1915. Einstein's theory of relativity generalizes Einstein's spacial theory of relativity and Newton's law of universal gravitation, providing a unified description of gravity as a geometrical property of space and time (or space-time). According to the Einstein field equations the curvature of space-time is directly associated with the mass, momentum and energy of the matter and/or radiation. In fact, the predictions of GR are extremely well tested within the "local" universe, both within the weak field limit (as in the Solar System) and more recently for strongly self-gravitating bodies in pulsar binary systems. General relativity theory has passed many tests, including scheme, binary pulsar, and cosmological ones. What all of those tests have in common is that they sample the quasi-stationary, quasi-linear weak-field regime of GR that's, they sample the regime of space-time where the field is weak relative to the mass-energy of the system, the characteristic velocities of gravitating bodies are small relative to the speed of light, and therefore the field is stationary or quasi-stationary relative to the characteristic size of the system [1]. Tests of general theory of relativity serve to ascertain observational evidence for the speculation of general theory relativity.

The largest deviations from GR are expected within the strongest gravitational fields around black holes (BHs), where different theories of gravity make significantly different predictions. The recent detection of gravitational waves by LIGO seems to indicate that even events related to very strong gravitational fields, like the merger of two stellar-mass BHs, fulfill the predictions of GR. This extremely exciting discovery entails additional verification using observations within the electro- magnetic spectrum. In fact, astronomical observations and gravitational wave detectors may soon provide us with the chance to review BHs very well, and to probe GR within the strong-field

regime, where tests are currently lacking.

The explore for gravitational waves has many motivations. First is easy, fundamental scientific curiosity about new phenomena. More prosaically, one can use gravitational radiation to check Einstein's general theory of relativity. for instance, one can test the expected transverse and quadrupolar nature of the radiation, and one can test whether or not the radiation travels at the speed of light, in concert would expect for a mass less graviton. One can even directly probe highly relativistic phenomena, like black hole formation. Perhaps more intriguing, though, is that the entirely new view one gains of the universe. Gravitational waves can not be appreciably absorbed by dust or stellar envelopes, and most detectable sources are a number of the foremost interesting and least understood objects within the universe. More generally, gravitational wave astronomy release a completely new non-electromagnetic spectrum [2].

Gravitational waves are traveling perturbations within the fabric of space-time from accelerating masses, very similar to electromagnetic waves are perturbations in electric and magnetic fields from accelerating charges. Gravitational waves are a natural consequence of the theory of general relativity(TGR). Einstein predicted the existence of them (Einstein 1916), but he also claimed that the perturbations would be so small that we must always not bother searching for them[3].

The GW measurements made by LISA will probe the most extreme and violent manifestations of gravity and thus are probably the best way to test the fundamental nature of gravity. In particular, GW test the theory of gravity in the limit of very high velocities (approaching the speed of light) and very strong space-time deformations. The two key factors that make LISA a very good instrument to test our current understanding in the form of Einstein's general relativity are the high signal-to-noise detection's and the in-spiral and merger of the two black holes. This complements the (most likely) earlier tests of general relativity using GWs from ground-based detectors such as LIGO/Virgo and the Einstein telescope. In the in-spiral phase of the detection, the measurements can be examined for evidence of a massive gravitation as predicted by several alternative gravity theories, that would show up as a frequency-dependent phase shift. In addition, the in-spiral phase can be compared in great detail with predictions from general relativity using numerical relativity simulations and thus expose any hints of the incompleteness

of general relativity. The merger and ring-down phases can be used again to test GR, because the accurate determinations of the masses and spins of the two black holes during in-spiral, together with numerical relativity simulations to predict the signature of the merger and the properties of the final remnant and compared directly with the observations. Finally, the properties of the ring-down, in general relativity, are completely determined by the pre-merger binary and the mass and spin of the final black hole, again providing a consistency check for general relativity. Gravitational-wave observations from binary coalescence and inference of source properties are made through waveform models built solving Einstein's field equations. Waveform models can also be built in theories of gravity alternative to GR [4].

Solving the complete Einstein equations on the computer is that the subject of numerical relativity, which could even be called computational theory of relativity. Computers also play a task in algebraic computations and in approximation schemes, and such calculations are important topics in numerical relativity. But the distinguishing feature of numerical relativity is that, in theory, the Einstein equations fully generality can and must be solved numerically. Numerical relativity spans an outside range of various topics including mathematical general relativity theory, astrophysics, numerical methods for partial differential equations, programming, and simulation science. Current research in numerical relativity is in a very transition from a self-contained topic in theoretical physics to a physical theory with numerous connections to observational astronomy [5].

In Our work we use the LIGO GW150914 data, linear approximation of Einstein field equations, effective one body formalism, in-spiral-Merge-Ring down Phenomenological wave model, numerical Relativity, python package and PyCBC catalogue.

The purpose of the PyCBC search is to identify gravitational wave signals from binary neutron star and black hole mergers and measure the statistical significance of candidate events. PyCBC is an open-source computer program bundle fundamentally composed within the Python programming dialect which is outlined for utilize in gravitational-wave cosmology and gravitational-wave data analysis. PyCBC contains modules for signal preparation, matched filtering, gravitational waveform generation, among other assignments common in gravitational-wave data analysis. The program is created by the gravitational wave community nearby LIGO and Virgo researchers to analyze gravitational wave data [6].

1.1 Objective of the thesis

1.1.1 General objective

To study gravitational waves which are one of verification of General Theory of Relativity.

1.1.2 Specific objectives

- Analyzing gravitational-wave signals by using Spin-Effective-One-Body-Numerical-Relativity(SEOBNR) and In-spiral-Merg-Ringdown phenomenological(IMRPhenom) models.
- Comparing gravitational wave detected by the LIGO and numerical relativity solution of general relativity to the SEOBNR and IMRPhenom models.

1.2 Thesis outline

The rest of the thesis is organized as follows. Chapter 2 deals with the theoretical background of general relativity and its foundation of the equivalence principle and the special relativity, the prediction of GR, direct and generic tests of general relativity. Source of gravitational wave, the properties of gravitational wave, the speed, the polarization and some use of gravitational wave are presented in this chapter.

Chapter 3 presents the methodology used to study in this thesis, derivation of Einstein field equation in empty space and linear approximation of gravity, the quadrupole formalism including the two body problem and effective one body models and also methods used in this thesis like; numerical relativity, and phenomenological waveform models are presented.

Chapter 4 presents discussion of results, this includes data analysis of gravitational wave with different parameters like; mass, frequency, distance from source and the agreement of LIGO gravitational wave signal to the phenomenological and SEOBNR wave models and also agreement to the general relativity simulated by numerical relativity. Finally, conclusions are presented in Chapter 5.

General theory of relativity and gravitational waves

2.1 Introduction

Einstein's theory of general relativity has passed a large number of tests over 100 years since its conception. The observation of gravitational waves emitted by two coalescing black holes was one in all the foremost accepted discoveries within the history of theory of relativity, and Einstein was proven right again. Einstein's general theory of relativity predicts the existence of gravitational waves, disturbances of space-time itself that propagate at the speed of light, and have two transverse quadrupolar polarization. Gravitational waves will allow us to find out about the gravitational interaction in regimes that are currently inaccessible by more conventional, electromagnetic means. Binary black hole and neutron star mergers, for example, cause gravitational fields that are intensely strong and highly dynamical, a regime where Einstein's general theory of relativity has not yet been tested [7]. In this chapter we will discuss the theory of GR and GWs.

2.2 General theory of relativity

General relativity rests on two foundation stones: the equivalence principle and special relativity.

2.2.1 Equivalence principle

According to the principle of equivalence, it is impossible to distinguish between the gravitational field and the acceleration reference system[8]. within the theory of Einstein's general theory of relativity, the equivalence principle is that the equivalence of gravitational and mass. It states that the result of any local non-gravitational experiment in a very freely falling laboratory is independent of the speed of the

laboratory and its location in space-time. Equivalence principle originates in Galileo's observation that every bodies fall in an exceedingly gravitational field with the identical acceleration, no matter their mass. From the trendy point of view, which means if an experimenter were to fall with the acceleration of gravity (becoming a freely falling local inertial observer), then every local experiment on free bodies would give the identical results as if there is no gravity at all: without the usual acceleration, the particles will move at a constant speed, and conserve energy and momentum. The principle of equivalence naturally leads to the view that gravity is geometry. If all bodies follow the identical trajectory, just looking on their initial velocity and position but not on their internal composition, then it's natural to associate the trajectory with the spacetime itself instead of with any force that depends on properties of the particle. The equivalence principle can only hold locally, that's in a very small region of space and for a brief time [7].

2.2.2 Special theory of relativity

The second cornerstone of general relativity is special relativity. Indeed, this is what caused the downfall of Newtonian gravity: as an immediate theory, Newtonian gravity changed into identify as out of date as soon as special relativity changed into accepted. Many of the most distinctive predictions of general relativity come from their Conforms to the special theory of relativity. General relativity consists of special relativity thru the equivalence principle: local freely falling observers see special relativity physics. That means, in particular, not anything moves faster than light, that mild moves on the same velocity c with respect to all local inertial observers on the identical event, and that phenomena like time dilation and the equivalence of mass and energy are a part of general relativity. Gravitational waves themselves are of course the result of the unique theory of relativity applied to gravity. Any alternate to a supply of gravity (e.g. the position of the star) must alternate gravitational fields, and this conversion cannot move outward faster than light. Far enough from the source, this transformation is only a ripple within side the gravitational field. In the general theory of relativity, this wave moves at the speed of light.. In principle, all relativistic gravitation theories have to encompass gravitational waves, despite the fact that they might propagate slower than light [7]. A general-relativistic space-time is a pair (M, g) where; M is a four-dimensional manifold; local coordinates will be denoted (x^0, x^1, x^2, x^3) and Einstein's summation convention will be used for Greek indices $\mu, \nu, \sigma, \dots = 0, 1, 2, 3$ and for latin indices $i, j, k, \dots = 1, 2, 3$.

g is a Lorentzian metric on M , i.e. g is a covariant second-rank tensor field. The metric contains all information about the space-time geometry and thus about the gravitational field.

$ds^2 > c^2 dt^2 \rightarrow$ space-like (A - C)

$ds^2 = c^2 dt^2 \rightarrow$ null (light cones)

$ds^2 < c^2 dt^2 \rightarrow$ time-like (A - B)

Where ds is flat spacetime and given by

$$ds^2 = -(cdt)^2 + dx^2 + dy^2 + dz^2 \quad (2.1)$$

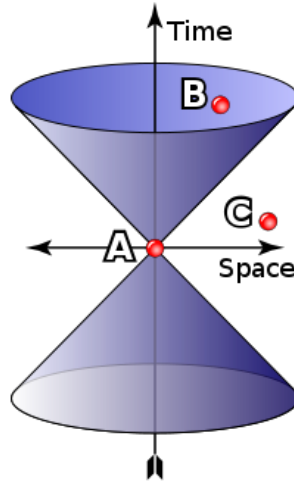


Figure 2.1: The causal structure of spacetime [10]

Time-like curves describe motion at subluminal speed and light-like curves describe motion at the speed of light. Space-like curves describe motion at superluminal speed which is forbidden for signals [9, 10]. General theory of relativity is a nonlinear theory. The laws of general relativity are described by Einstein's field equations at any point x on a four-dimensional manifold (which we shall call spacetime) with $x = (x^0 = ct, x^1, x^2, x^3)$, t denotes the time coordinate.

$$R_{\mu\nu} - \frac{1}{2}g_{\mu\nu}R = \frac{8\pi G}{c^4}T'_{\mu\nu} \quad (2.2)$$

or equally (taking the trace and replacing R with T),

$$R_{\mu\nu} = \frac{8\pi G}{c^4} \left(T_{\mu\nu} - \frac{1}{2}g_{\mu\nu}T \right). \quad (2.3)$$

Here, c is the speed of light, G is Newton's gravitational constant, $R_{\mu\nu} = R^{\sigma}_{\mu\sigma\nu}$ is the Ricci tensor, $R = R_{\mu\nu}g^{\mu\nu}$ is the Ricci scalar, $T_{\mu\nu}$ is the energy-momentum tensor

which gives the energy density, $T_{\mu\nu}U^\mu U^\nu$ for any observer field with 4-velocity U^μ normalized to $g_{\mu\nu}U^\mu U^\nu = -c^2$. To our present understanding, all physical processes in the macroscopic universe are governed by these equations. The left-hand side of Eq.2.3 renders information about the local curvature of spacetime while the right-hand side incorporates the local energy-momentum density [9, 11, 12].

Einstein's theory has passed each test or observational test it has ever been subjected to. One of the predictions of general relativity was gravitational waves. In reality, Einstein himself came up with this expectation only a year afterward in 1916. According to general relativity, gravity is portrayed by the ebb and flow of spacetime [13]. General relativity is our current prevailing description of gravity. GR describes gravity as a geometric property of spacetime, the four-dimensional fabric of our Universe. The curvature of spacetime is dictated by the energy, momentum, and angular momentum of the matter present. And in response, the evolution of the matter is dictated by the curvature of spacetime. As John Wheeler eloquently put it: "Spacetime tells matter how to move; matter tells spacetime how to curve." For example, when the Earth orbits the Sun, according to GR it is not being pulled by a gravitational force, but instead is merely following the straightest possible path in the curved spacetime around the Sun [14].

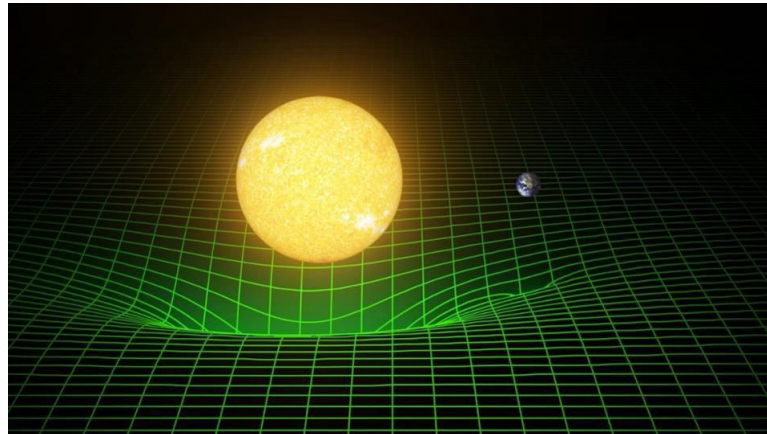


Figure 2.2: The curvature of space-time caused by the sun and the earth, represented by a grid. The spacetime around the Sun is warped due to its mass. The Earth then merely follows a geodesic, or a locally straight path, in this curved spacetime. However, since the spacetime itself is curved, this locally straight path becomes a curved path on a global scale; an ellipse in this instance. The Earth also warps the spacetime around itself, which causes the Moon to orbit it [14].

As it were view points of GR required to accepted the presence of gravitational-waves are that information cannot travel faster than the speed of light which mass bends space-time. Consider two black holes, each irritating space-time, orbiting around each other. The curvature at any specific point in space must alter in reaction to the moving mass, but the space- time distortion cannot travel faster than the speed of light. The gravitational wave is the changing curvature engendering through space-time, a perturbation within the metric transmitting the news that the mass has moved.

2.2.3 Prediction of general relativity

The main predictions of Einstein's general theory of relativity includes: perihelion precession of Mercury, bending of light(gravitational lensing), the existence of black holes, gravitational waves from compact object. All this tests of general relativity which incorporate solar system tests and tests concerning double pulsars, deal with the regime where the gravitational fields are weak, speeds are small, and particles are quasi-static. Our concern in this thesis is gravitational wave test of general relativity. When electrons vibrate, how electromagnetic force emits light; in general relativity, when we shake massive objects, gravitational waves are also generated. For the first time, gravitational wave perception of binary black hole coalescence given us with an opportunity to test gravity and test general relativity within the strong field, large velocity and a highly dynamical regime which was blocked off sometime recently. These waves carry information about black holes that cannot be obtained by other means, because the telescope cannot see non-luminous objects. For each event, we are able to measure the black hole, masses, their rate of rotation or "spin," and details about their locations and orientations with varying degrees of certainty. This information allows us to find out how these objects formed and evolved in cosmic time. General relativity tells us that, among other things, some stars can become so dense that they are isolated from the rest of the universe. These extra ordinary objects are called black holes. General relativity also predicted that when pairs of black holes orbit tightly around each other in a binary system, they stir up space-time, the very fabric of the cosmos. This disturbance of space-time that sends energy across the universe in the form of gravitational waves. That loss of energy causes the binary to tighten further, until eventually the two black holes smash together and form a single black hole. This spectacular collision generates more energy in gravitational waves than all stars in the universe combined, and more energy than light [3, 13].

2.3 Direct and generic tests of general relativity

Gravitational-wave tests of Einstein's theory can be classed into two distinct subgroups: direct tests and generic tests.

2.3.1 Direct test

Direct testing follows a top-down approach, starting with specific modifications. The gravitational theory of known action, deriving and solving modified field equations. They are used in specific gravitational wave radiation systems. Direct testing is a standard method for testing general relativity with gravitational wave, inside the prototype here is a test of Jordan Fier-Brans-Dicke theory, other Examples of direct testing include testing of a modified secondary gravity model. And non-commutative geometry theory[1].

2.3.2 Generic tests

Generic tests adopt a bottom-up approach, where one takes a particular feature of GR and asks what type of signature its absence would leave on the gravitational-wave observable; one then asks whether the data presents a statistically-significant anomaly pointing to that particular signature [1].

2.4 Gravitational waves

Einstein's general theory of relativity predicts that a dynamic system in a strong gravitational field will release a large amount of energy in the form of gravitational radiation. These gravitational "waves" are among the most elusive signals from the deepest reaches in the Universe. They can be thought of as ripples in the curvature of spacetime [14].

Gravitational waves are disturbances in the curvature of space-time, generated by accelerated masses, that propagate as waves outward from their source at the speed of light. In Einstein's theory of general relativity, the geometry of space-time is a dynamic physical observable that supports wave-like excitation, propagating at the speed of light. These are known as gravitational waves; their elementary excitation, or normal modes, have the properties of mass less, spin 2 particles with two linearly independent polarization states they are called gravitation. Like all sorts of waves, gravitational waves carry the energy and in fact transport, it away

from the source. In this process, since energy is preserved, the binary system is losing energy. In a Newtonian description, the energy of our binary system is given by

$$E = \frac{1}{2}M \left(\frac{a}{2}\Omega\right)^2 \times 4 - \frac{GM^2}{a} = -\frac{GM^2}{2a} \quad (2.4)$$

where the last form follows from Kepler's third law, $\Omega^2 a^3 = G(M_1 + M_2)$. The loss of energy from the binary leads to a reduction in the separation a , or in-spiral. It is clear that this is a run-away process: the closer they get together, the more they radiate; and the more they radiate, the closer they get together. In general relativity, binary systems are inherently unstable and undergo a slow in-spiral and eventual merger to a single object [15].

2.5 Sources of gravitational waves

The two primary categories of gravitational waves sources for LISA are the galactic binaries and therefore the massive black holes (MBHs) expected to exist within the centers of most galaxies. Because the masses involved in typical binary systems are small (a few solar masses), the observation of binaries is proscribed to our galaxy. Galactic sources which will be detected by LISA include a large sort of binaries, such as pairs of close white dwarfs, pairs of neutron stars, neutron star and black hole (5-20 M_\odot) binaries, pairs of contacting normal stars, normal star and white dwarf star (cataclysmic) binaries, and possibly also pairs of black holes [7].

In spite of the fact that each accelerating non-symmetric system emanates GWs, as it were the ones that are able to perturb the metric enough can be detected with current innovation. Actually, we are looking for those frameworks that are massive, compact, and/or violent enough to actuate a sufficiently strong gravitational field. It turns out that such sources are as it were of astrophysical origins, such as black holes (BHs) and neutron stars (NSs) or violent events like supernovae and gamma-ray bursts. In this area, we are going to see a few of the foremost promising sources for detection by ground-based detectors [16].

2.5.1 Compact binary coalescence

Binary system are composed of two objects orbiting around their common center of mass. When black holes orbiting each other, an outer ring of gas surrounds the whole system and mini disk surrounds each black hole, streams of gas connect the disks, so that magnetic and gravitational forces heat up the gas producing UV

and x-ray light, the amount of gas flowing in the system and our viewing angle can alter what we will see, intense gravity bends space time. The light follows warped path and is distorted as with a lens. this also creates an "eyebrow" next to one black hole caused by light from glowing gas immediately out side the other. Compact binary coalescence (CBC) may be a class of sources during which two

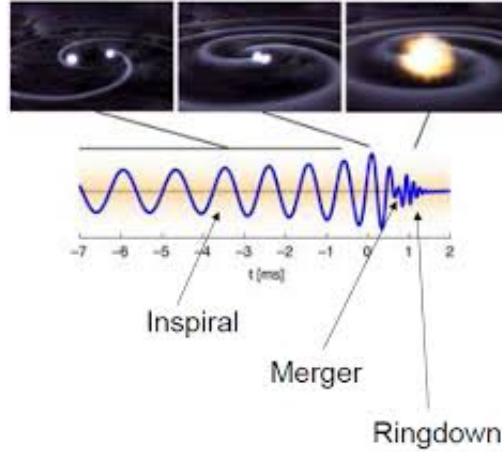


Figure 2.3: Orbits of binary system around their comen center of masses [17].

compact objects, either a NS or a BH, orbit around one another. CBC sources are further subdivided into binary neutron star (BNS), black hole neutron star(BHNS) and binary black hole (BBH). The emission of GWs carries energy and momentum off from the system, causing the two objects to spiral towards one another. the foremost famous CBC system is probably the Hulse-Taylor binary pulsar. The orbital evolution of the Hulse-Taylor binary pulsar provided the primary evidence of the emission of GWs [16]. The phenomenon bringing these system to coalescence is that the back-reaction in in-spiraling systems. The energy emitted influences the source motion, and successively the new motion affect the GW emission. within the quadrupolar approximation the change in frequency is given by:

$$\frac{d \ln(f_{gw})}{dt} = 0.126 \left(\frac{M_c}{M_\odot} \right)^{5/3} \left(\frac{f_{gw}}{100Hz} \right)^{8/3} \quad (2.5)$$

and then the frequency before coalescence is given by:

$$f_{gw}(t) \simeq 134Hz \left(\frac{1.21M_\odot}{M_c} \right)^{5/8} \left(\frac{1s}{\tau} \right)^{3/8} \quad (2.6)$$

Where $\tau = (t_{coal} - t_{ret})$ is the time remaining before coalescence, t_{coal} denotes time of coalescence and t_{ret} is retarded time. We define also the chirp mass M_c [18]:

$$M_c = \frac{(m_1 m_2)^{3/5}}{(m_1 + m_2)^{1/5}} \quad (2.7)$$

Where m_1 and m_2 are mass of black hole one and black hole two. The chirp indicates that as gravitational waves are emitted, they carry energy faraway from the binary. The gravitational binding energy decreases, and also the orbital frequency increases. one among the simplest samples of CBC source of gravitational waves are black holes. Black holes are one of the most imperative sources of gravitational waves. For the case, it's assumed that matter being gulped by a black hole can produce this kind of waves. looking at Eq.2.8, the fact that the radius is raised to a power of -5 tells us that when matter reaches the black hole it can emit a robust burst.

$$L_{GW} \sim \left(\frac{GM}{Rc^2} \right)^5 L_0 \quad (2.8)$$

It has been estimated that the energy out-put E of such burst would be;

$$E \approx \frac{0.0104m^2}{M} c^2. \quad (2.9)$$

m being the mass of the matter falling, and M the mass of the black hole. However, matter falling into black holes is not the only way for black holes to emit gravitational waves. If there are two massive black holes colliding against each other, they will also produce radiation [19]. GWs from CBC sources can be divided into three stages, the in-spiral, the merger and the ring down phase.

a) *In-spiral phase*

The in-spiral is the orbit of two bodies about a common center of mass where in the orbital radius decreases with time due to energy loss from sources including gravitational radiation [20]. The in-spiral stage lends itself to a natural perturbation approach. To illustrate with a simple, concrete example, consider two stars of equal mass M in a circular orbit of instantaneous radius $R(t)$ and angular velocity $\omega(t)$ (assumed slowly changing), where the stars are treated as point masses far enough apart that tidal effects can be neglected. From simple Newtonian mechanics, we obtain Kepler's 3rd Law:

$$M\omega^2 R = \frac{GM^2}{(2R)^2} \Rightarrow \omega^2 = \frac{GM}{4R^3} \quad (2.10)$$

The total energy of this system (potential + kinetic) is

$$E = -\frac{GM^2}{2R} \quad (2.11)$$

and the decrease in E with time is

$$\frac{dE}{dt} = \frac{GM^2}{2R^2} \frac{dR}{dt} \quad (2.12)$$

as the orbit shrinks.

For convenience, gravitational wave signal for different mass of binary system for the IMRPhenomB model. We see that the amplitude, as well as the frequency are modified, from the in-spiral to the ring-down phase. The left panel constructed from two equal masses of black holes the amplitude of wave is small compared to the right one. The right panel one mass of the black hole kept fixed ($10 M_{\odot}$) whereas the second masses free to change. We define the origin at the orbit's center and the $x - y$ plane to coincide with the orbital plane, with one star at $x_1 = R$ at time $t = 0$:

$$x_1(t) = -x_2(t) = R \cos(\omega t); \quad y_1(t) = -y_2(t) = R \sin(\omega t); \quad z_1 = z_2 = 0 \quad (2.13)$$

using equations $I^{ij} = \int d^3x \mu(t, \vec{x}) x^i x^j$ and $\tilde{I}^{ij} = I^{ij} - \frac{1}{3} \delta^{ij} I^k_k$, for the total energy luminosity for waves in the radiation zone depends on the third time derivative of a modified inertia tensor \tilde{I}^{ij} :

$$L = \frac{G}{5c^5} \langle \ddot{\tilde{I}}_{ij} \ddot{\tilde{I}}^{ij} \rangle \quad (2.14)$$

where $\langle \rangle$ represents an average over several cycles, and I is the trace-less quadrupole tensor:

$$L = \frac{128}{5} \frac{GM^2}{c^5} R^4 \omega^6 \quad (2.15)$$

Notice that the expression for L_{gw} is dimensionless when $c = G = 1$. It can be converted to normal luminosity units by multiplying by the scale factor $L_0 = c^5/G = 3.6 \times 10^{52}$ W. This is an enormous luminosity. By comparison, the luminosity of the sun is only 3.8×10^{26} W, and that of a typical galaxy would be 10^{37} W. All the galaxies in the visible universe emit, in visible light, on the order of 10^{49} W. We will see that gravitational wave systems always emit at a fraction of L_0 , but that the gravitational wave luminosity can come close to L_0 and can greatly exceed typical electromagnetic luminosity. Close binary systems normally radiate much more energy in gravitational waves than in light. Black hole mergers can, during their peak few cycles, compete in luminosity with the steady luminosity of the entire universe! [21] putting $dE/dt = -L$ and using Eq.2.10, one obtains a differential equation for R

$$R^3 \frac{dR}{dt} = -\frac{4}{5} \frac{G^3 M^3}{C^5} \quad (2.16)$$

Integrating from a present time t to a future coalescence time t_{coals} when $R \rightarrow 0$, one finds the orbital radius [2].

$$R(t) = \left[\frac{16}{5} \frac{G^3 M^3}{c^5} (t_{coal} - t) \right]^{\frac{1}{4}} \quad (2.17)$$

The signals that the simplest waveform predictions are available have well-defined frequencies. In some cases the frequency is dominated by an existing motion, like the spin of a pulsar. But in most cases the frequency are going to be associated with the natural frequency for a self-gravitating body, defined as

$$\omega_0 = \sqrt{\pi G \bar{\rho}} \quad \text{or} \quad f_0 = \omega_0/2\pi = \sqrt{\frac{G \bar{\rho}}{4\pi}} \quad (2.18)$$

where $\bar{\rho}$ is the mean density of mass-energy in the source. This is of the same order as the binary orbital frequency and the fundamental pulsation frequency of the body. The mean density and hence the frequency are determined by the size R and mass M of the source, taking $\bar{\rho} = 3M/4\pi R^3$. For a neutron star of mass $1.4 M_\odot$ and radius 10 km, the natural frequency is $f_0 = 1.9$ kHz. For a black hole of mass $10 M_\odot$ and radius $2M = 30$ km, it is $f_0 = 1$ kHz. And for a large black hole of mass $2.5 \times 10^6 M_\odot$, such as the one at the center of our galaxy, this goes down in inverse proportion to the mass to $f_0 = 4$ mHz. In general, the characteristic frequency of the radiation of a compact object of mass M and radius R is [21]

$$f_0 = \frac{1}{4\pi} \left(\frac{3M}{R^3} \right)^{1/2} \simeq 1 \text{kHz} \left(\frac{10M_\odot}{M} \right) \quad (2.19)$$

from which the gravitational wave frequency [$f_{GW} = \omega/2\pi$] is derived via Eq.2.10.

$$f_{GW} = \frac{1}{8\pi} [2.5^3]^{1/8} \left[\frac{c^3}{GM} \right]^{5/8} \frac{1}{(t_{coal} - t)^{3/8}} \quad (2.20)$$

As expected, the frequency diverges as $t \rightarrow t_{coal}$. Now consider the amplitude h_0 of the circularly polarized wave observed a distance r away along the orbital axis of rotation is:

$$h_0(t) = \frac{1}{r} \left[\frac{5G^5 M^5}{2c^{11}} \right] \frac{1}{(t_{coal} - t)^{1/4}} \quad (2.21)$$

Note that if the distance to the source is known, the common stellar mass of this system can be derived from either the frequency or amplitude evolution [2].

b) Merger phase

Merger phase is a short-lived stage that takes after the in-spiral stage and happens when the two objects are so near to each other that they begin to merge into a single object. The gravitational fields are now very strong and the GW emission can as it were be computed by considering the complete EFE numerically. Because it turns out, the merger stage can cause a GW emission that surpasses the electromagnetic emission of the whole Universe. Once the two objects have merged and formed a single object, it will further emit GWs as the object tries to reach a quiescent state.

The GWs emitted during this phase can be described by a superposition of damped sinusoidal, also referred to as quasi-normal modes [16].

c) Ringdown phase

The ultimate black hole that's formed as a result of a merger is usually within the excited state. The deformations of the black hole faraway from the stationary Kerr setups are radiated away. The perturbations pass away down because of the emission of gravitational waves and therefore the waveform looks just like the superposition of damped sinusoidal. This stage is understood as the ring down [13, 22].

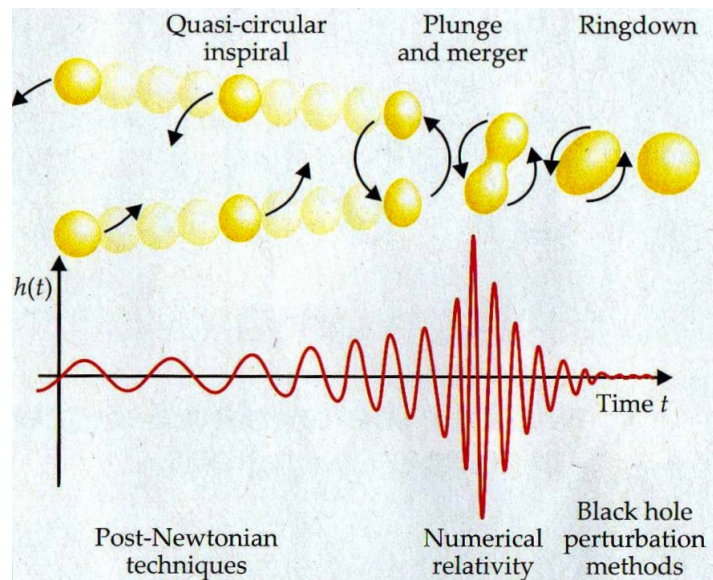


Figure 2.4: Coalescence of binary black holes. The loss of energy and angular momentum via the emission of gravitational radiation drives compact-binary coalescence, which proceeds in three different phases. The strongest gravitational-wave signal, illustrated here because the gravitational-wave amplitude h , accompanies the late in-spiral phase and therefore the plunge and merger phase; for that a part of the coalescence, post-Newtonian and perturbation methods break down, and numerical simulations must be used [23].

2.5.2 Continuous wave sources

Continuous-wave (CW) sources are those that emit GWs with generally constant frequency and amplitude compared to the recognition time. The prime candidates to emit such signals are quickly rotating, non-asymmetric NSs. Such deformations can emerge due to, for example, strain build-up within the crust or within the core, or growth of matter. The GW signal from CW sources is relatively simple due to

their slow variation of amplitude and frequency. Although the GW amplitude is generally weaker compared to CBC sources, a longer integration time means that CW sources may also achieve detectable SNR. Finally, the analysis of such sources can be simplified if some of its characteristics can be determined through means other than GWs, e.g. rotational frequency of an NS through the observation of a pulsar [16].

2.5.3 Burst sources

Burst sources are related to galactic temporal phenomena, such as supernovae, gamma-ray bursts, or instabilities in NSs. Supernovae happen when massive objects collapse under the impact of gravity. At the end of their lives, some stars collapse on themselves because of their gravity fields and generate core-collapse supernovae of type Ib, Ic, or II. If this process deviates from spherical symmetry, it can create gravitational waves. The physics of core-collapse supernovae is highly complex and contains a lot of different factors (electromagnetic fields, neutrino physics, relativistic hydro-dynamical shock fronts, general relativity effects) and their modeling heavily relies on numerical simulations [24]. Estimations say that the power output of the explosion of a star of mass M is

$$E \approx 0.1Mc^2. \quad (2.22)$$

However, a large part of this probably happens through neutrino emission. Supernovae are a good gravitational source. They are compact and have large accelerations. Initial density and temperature fluctuations and other factors may direct asymmetric collapse. If a supernova, which is exceptionally bright, is observed in gravitational wave, we will be able to test a prediction of general relativity which states that the speed of gravitational wave is the same speed as light [19]. Within the process that follows, NSs or BHs are formed, and GWs are radiated through dynamical processes. On the opposite hand, GRBs are flashes of gamma-rays, that the progenitors are still uncertain. Possible progenitors are supernova-like events (causing future delicate spectrum GRBs, moreover called long delicate GRBs) additionally as the merger of compact objects (causing brief hard GRBs). These sources are generally difficult to model due to the complicated physics associated with such phenomena. Therefore, the explore for GWs from such sources often happens with unmodeled filters, where unmodeled implies that there's no astrophysical model related to the GW. An example of such a filter may be a sine-Gaussian signal [16].

For scale, consider a supernova a distance r away in our galaxy that emits energy E in gravitational waves, with a characteristic duration T and characteristic frequency f . One expects a detectable strain amplitude at the Earth of about;

$$h \sim 6 \times 10^{-21} \left(\frac{E}{10^{-7} M_{\odot} c^2} \right)^{\frac{1}{2}} \left(\frac{1ms}{T} \right) \left(\frac{1kHz}{f} \right) \left(\frac{10kpc}{r} \right) \quad (2.23)$$

expression, the initial LIGO interferometric ought to have been able to detect a galactic supernova in gravitational waves. But no supernova was detected electromagnetically in our galaxy during initial LIGO data taking. One interesting situation in which a core-collapse supernova may be seen in gravitational waves to much bigger separations is through a bar mode instability, in which differential rotation in a collapsing star leads to a huge, rapidly spinning quadrupole moment, generating waves detectable from well exterior our own galaxy. An other sort of instability (r-mode) may develop within the birth of a neutron star, but its lifetime is expected to be long enough. An other potential temporal source of ineffectively known gravitational waveform shape is the sudden release of vitality from a profoundly magnetized neutron star (magnetar). In spite of the fact that "conventional" neutron stars are characterized by extremely strong surface magnetic fields ($\sim 10^{12}G$), many magnetars appear to have fields $\sim 100 - 1000$ times still stronger, implying enormous pent-up magnetic energy. It is thought that soft gamma-ray repeaters (SGRs) and anomalous X-ray pulsars (AXPs) are different observational manifestations of the identical underlying system a highly magnetized star which sporadically converts magnetic field energy into radiation. An other possible transient source is an emission of bursts of gravitational radiation from "cosmic string cusps". Cosmic strings could be defects remaining from the electroweak (or earlier) state change or possibly primordial super strings red shifted to enormous distances. A general consideration in burst searches is that the energy release implicit for a given source distance and detectable strain amplitude. As the distance of the source increases, the energy required for its waves to be detectable on Earth increases as the square of the distance. Specifically, rewriting Eq.2.23, one obtains the relation:

$$E \sim (3 \times 10^{-3} M_{\odot} c^2) \left(\frac{h}{10^{-21}} \right)^2 \left(\frac{T}{1ms} \right) \left(\frac{f}{1kHz} \right) \left(\frac{r}{10Mpc} \right)^2 \quad (2.24)$$

Hence for a source distance much beyond $10Mpc$ and for initial LIGO sensitivities to transients, one needs sources emitting significant fractions of a solar mass in gravitational radiation in frequency bands accessible to terrestrial detectors, such as is expected in the case of coalescing binary systems [2].

2.5.4 Stochastic background

Stochastic background comes from the density fluctuation of the early stage of the universe and the superposition of numerous unresolved GW sources. Measuring the background would tell us about the nature of the Planck-size universe and provide clues for testing the various cosmological models. Although stochastic background is interesting, it is so weak that modern technology is far from achieving this task. It is divided into two classes: the primordial background and the astrophysical background. The primordial background consists of radiation originating from the early Universe, such as the Big Bang. The astrophysical background comes from the GW radiation from astrophysical sources such as CBC systems or cosmic-string cusps and kinks. The detection of a stochastic background is some what different compared to the sources described above. Since random radiation is indistinguishable from instrumental noise, at least for short observation times, it cannot be detected with a single detector. Instead, the output of several detectors are combined to calculate the cross-correlation between detectors. An excess in the cross-correlation can then be an indication of a stochastic background [16].

A primordial isotropic gravitational wave background is predicted by most cosmological theories, although the predicted strengths of the background vary enormously. It is customary to parametrize the background strength versus frequency f by its energy density per unit logarithm normalized to the present-day critical energy density $\rho_{crit} = 3H_0^2 c^2 / 8\pi G$ of the universe, where H_0 is Hubble's constant, taken here to be 70.5 km/s/Mpc

$$\Omega_{gw}(f) = \frac{1}{\rho_{crit}} \frac{d\rho_{gw}(f)}{d\ln(f)} \quad (2.25)$$

The associated power spectral density can be written

$$S_{GW} = \frac{3H_0^2}{10\pi^2} f^{-3} \Omega(f) \quad (2.26)$$

Note that, for the cosmic microwave background radiation, the primordial gravitational waves would be highly red-shifted from the expansion of the universe, but likely to a much greater degree, since they would have decoupled from matter at vastly earlier times. A more convenient reformulation in amplitude spectral density can be written as:

$$h(f) = [S_{GW}(f)]^{\frac{1}{2}} = (5.6 \times 10^{-22}) h_{100} (\Omega(f))^{\frac{1}{2}} \left(\frac{100 \text{ Hz}}{f} \right)^{\frac{3}{2}} \text{ Hz}^{-\frac{1}{2}} \quad (2.27)$$

where $h_{100} \equiv H_0 / (100 \text{ km/s/Mpc})$.

A key question is what range of values are expected for $\Omega(f)$? Fig.2.5 shows a range of expectations versus frequency (28 orders of magnitude in frequency and 12 in Ω). The bottom curve is a rough estimate expected from standard inflationary scenarios. This graph also shows direct limits on gravitational wave energy density from comparison of observed abundances of elements with predictions from Big Bang nucleosynthesis (BBN), in addition to limits derived from measurements of anisotropies in the CMBR. For reference, the normalized total energy density of the CMBR itself is about $\Omega_{CMBR} = 5 \times 10^{-5}$, and the energy density from primordial neutrinos is estimated to be bounded by $\Omega_{\nu\bar{\nu}} < 0.014$. The $\Omega(f)$ sensitivity of the initial LIGO and Virgo detectors to this isotropic background is 10^{-6} , with an expected improvement of more than three orders of magnitude for advanced detectors [2].

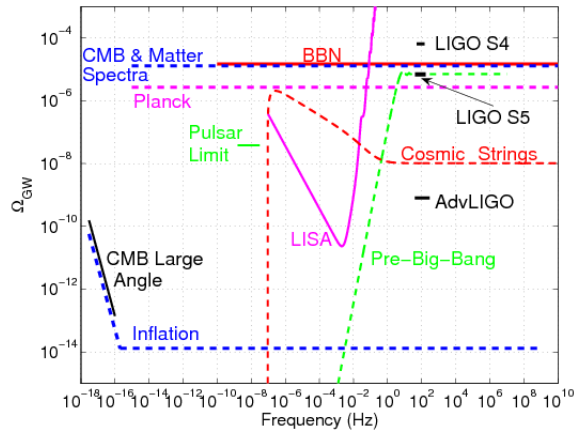


Figure 2.5: Comparison of different stochastic gravitational wave background measurements and models [2].

2.6 Gravitational radiation as a tool for testing general relativity

2.6.1 Tests of scalar-tensor gravity

Scalar-tensor theories generically predict dipole gravitational radiation, in addition to the standard quadrupole radiation, which results in modifications in gravitational-radiation back-reaction, and hence in the evolution of the phasing of gravitational waves from in-spiraling sources. The effects gives a more detailed picture of the SNR in the detectors around the time of the event. One clearly sees the presence of two peaks in the signal with a time delay between them corresponding to the

time needed for the wave to travel from one detector to the other, from the second figure we see that the gravitational wave is first detected in Livingston detector. For both sets of parameters, we see that the two LIGO detectors present a clear peak above the noise. are strongest for systems involving a neutron star and a black hole. Binary neutron star systems are less promising because the small range of masses near $1.4M_{\odot}$ with which they seem to occur results in suppression of dipole radiation by symmetry. Binary black-hole systems turn out to be observationally identical in the two theories, because black holes by themselves cannot support scalar "hair" of the kind present in these theories. Dipole radiation will be present in black-hole neutron-star systems, however, and could be detected or bounded via matched filtering. Interesting bounds could be obtained using observations of low-frequency gravitational waves by a space-based LISA-type detector. For example, observations of a $1.4M_{\odot}$ NS in-spiraling to a 10^3M_{\odot} BH with a signal-to-noise ratio of 10 could yield a bound on ω between 2.1×10^4 and 2.1×10^5 , depending on whether spins play a significant role in the in-spiral [25].

Scalar-tensor theories are very popular in unification schemes such as string theory or quantum gravity. Moreover, scalar fields are used to provide a model for cosmological inflation. In addition to the metric tensor, such theories contain a scalar function $\varphi(x)$ that can be incorporated into the Einstein-Hilbert action using minimal coupling, where a potential $V(\varphi)$ and a coupling function $A(\varphi)$ are used [12].

$$S = \frac{1}{16\pi} \int d^4x \sqrt{-g} [R - 2(\partial^\mu \varphi)(\partial_\mu \varphi) - V(\varphi)] + S_m[\psi_m, A^2(\varphi)g_{\mu\nu}]. \quad (2.28)$$

This expression is in the so-called Einstein frame, and in it, $g_{\mu\nu}$ is not the physical metric. In this expression, φ represents the scalar field, $V(\varphi)$ is a potential function, ψ represents the matter degrees of freedom, and S_m is the action for matter. In order to place this theory in the more intuitive frame in which the metric governs space-time separations, the Jordan frame, it can be re-written by making the conformal transformation $\bar{g}_{\mu\nu} = A^2(\varphi)g_{\mu\nu}$. In this new frame, $\bar{g}_{\mu\nu}$ is the physical metric, and the action takes the form

$$S = \frac{1}{16\pi} \int d^4x \sqrt{-g} [\phi R - \frac{\omega(\phi)}{\phi} (\partial^\mu \phi)(\partial_\mu \phi) - \phi^2 V] + S_m, \quad (2.29)$$

The new scalar field is represented by ϕ , where $\phi \equiv A^{-2}$, and $\omega(\phi)$ is called the coupling field. When this field is constant, i.e. $\omega(\phi) = \omega_{BD}$, this theory reduces to mass-less Jordan-Fierz-Brans-Dicke (Brans-Dicke) theory. In mass-less Brans-Dicke theory weak-field agreement with GR is recovered in $\omega_{BD} < 1/40000$. This

bound is set by tracking data from the Cassini spacecraft. More generally, scalar-tensor theories of this form, barring a certain class that are described by homogeneous solutions to the scalar field evolution equations, recover GR in the limit that $\omega \rightarrow \infty$ [26].

2.6.2 GR from in-spiral-merger-ring down consistency test

For the first time, gravitational wave observation of binary black hole coalescence provided us with an opportunity to probe gravity and test general relativity in the strong field, large velocity and highly dynamical regime which was inaccessible before [13].

To quantify the consistency of the observed signal with a binary black hole system predicted by GR, we define two parameters that describe the fractional difference between the two estimates of the remnant's mass and spin [27].

$$\epsilon := \frac{\Delta M_f}{\bar{M}_f}, \quad \sigma := \frac{\Delta a_f}{\bar{a}_f} \quad (2.30)$$

where

$$\Delta M_f := M_f^I - M_f^{MR}, \quad \Delta a_f := a_f^I - a_f^{MR} \quad (2.31)$$

and

$$\bar{M}_f := \frac{M_f^I + M_f^{MR}}{2}, \quad \bar{a}_f := \frac{a_f^I + a_f^{MR}}{2} \quad (2.32)$$

The best-fit general relativity waveform was subtracted from the detector output and it was checked whether the residual was in line with pure noise or there was leftover power. it had been found that the residual was indeed consistent with Gaussian noise. general relativity theory was tested to 4% level using this test, in other words the correlation between the detector output and also the waveform based on general relativity theory is larger than 96%. the ultimate mass and final dimensionless spin parameters of the remnant part, M_f and a_f can be determined in two ways, by using the in-spiral or low frequency part and by using the post-in-spiral or high frequency a part of the signal. within the case of GW150914 the critical frequency was 132 Hz. so as to work out the mass and spin of the remnant black hole input from the numerical relativity is required. Numerical relativity evolution starting from the information of the in-spiral phase allows us to predict the final mass and spin of the remnant black hole assuming Einstein's general theory of relativity. The dark purple color in Fig.2.6 confines the 90% confidence region in the $M_f - a_f$ plane based on the prediction using inspiral

part of gravitational waveform and numerical relativity. On the other hand, the dotted purple curve confines 90% confidence region based on the post-inspiral part of signal. The post-inspiral part of the signal contains merger and ringdown. Again using the numerical relativity fitting formulae the confidence region is inferred. It is clear from Fig.2.6 that two contours show significant overlap confirming that the two independent predictions of general relativity are indeed mutually consistent [13]. The left figure shows The final dimensionless spin a_f is plotted against

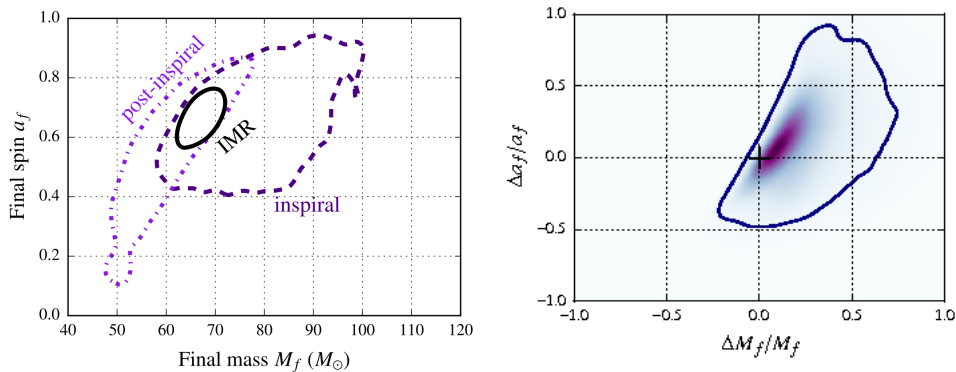


Figure 2.6: The right panel describe Posterior distributions for the parameters $\Delta M_f/M_f$ and $\Delta a_f/a_f$ that describe the fractional difference in the estimates of the final mass and spin from in-spiral and post-in-spiral signals. The contour shows the 90% confidence region. The plus symbol indicates the expected GR value (0, 0) [28]. There is a significant overlap. (Image credit: LIGO)

the final mass M_f in units of solar mass. The dark purple curve confines the 90% confidence region of the prediction of the final mass and spin based on the general relativistic numerical relativity simulation starting from the information from the in-spiral part of the gravitational wave signal. The dotted purple curve encloses 90% confidence region of the prediction of final mass and spin from the post-inspiral part of the gravitational wave signal. The solid black curve represents the prediction of the final mass and spin based on the full in-spiral-merger-ring down waveform [13].

2.7 Properties of gravitational waves

Gravitational waves, once they're generated, propagate almost unimpeded. Indeed, it's been proven that they're even harder to stop than neutrinos! the sole significant change they suffer as they propagate is that the decrease in amplitude while they travel far from their source, and also the Doppler shift they feel (cosmological, gravitational or Doppler), as is that the case for electromagnetic waves. There are other impacts that possibly impact the gravitational waveform, as an case,

assimilation by inter-stellar or inter-galactic matter mediating between the observer and also the source, which is extremely weak (actually, the extremely weak coupling of gravitational waves with matter is that the main reason that gravitational waves haven't been observed). Scattering and dispersion of gravitational waves also are practically unimportant, although they will be important during the first phases of the universe (this is additionally true for the absorption). Gravitational waves will be focused by strong gravitational fields and can also be diffracted, exactly as it happens with the electromagnetic waves. Gravitational waves are fundamentally different, however, while they share similar wave properties far from the source. Gravitational waves are transmitted by coherent bulk movements of matter (for case, by the implosion of the core of a star amid a supernova blast) or by coherent motions of space-time curvature, and thus they serve as a search of such phenomena. In contrast, cosmic electromagnetic waves are mainly the results of incoherent radiation by individual atoms or charged particles. Strong gravitational waves, are emitted from regions of space-time where gravity is incredibly strong and also the velocities of the bulk motions of matter are near the speed of light [29].

2.7.1 Polarization of gravitational waves

A laser-interferometric or resonant bar gravitational-wave detector measures the local components of a symmetric 3×3 tensor which consists of the "electric" components of the Riemann tensor, R_{0i0j} . These six independent components may be expressed in terms of polarization (modes with specific transformation properties under null rotations). Three are transverse to the direction of propagation, with two representing quadrupolar deformations and one representing an asymmetric "breathing" deformation. Three modes are longitudinal, with one an axially symmetric stretching mode within the propagation direction, and one quadrupolar mode in each of the two orthogonal planes containing the propagation direction. general theory of relativity predicts only the first two transverse quadrupolar modes, independently of the source, while scalar-tensor gravitational waves can in addition contain the transverse breathing mode. More general metric theories predict up to the full complement of six modes. an appropriate array of gravitational antennas could delineate or limit the quantity of modes present in an exceedingly given wave. If distinct evidence were found of any mode apart from the two transverse quadrupolar modes of GR, the result would be disastrous for GR. On the opposite hand, the absence of a breathing mode wouldn't necessarily rule out scalar-tensor gravity, because the strength of that mode depends on the character of the source [25].

2.7.2 Speed of gravitational waves

According to GR, within the limit during which the wavelength of gravitational waves is small compared to the radius of curvature of the background spacetime, the waves propagate along null geodesics of the background spacetime, i.e. they have the same speed, c as light. In other theories, the speed could differ from c due to coupling of gravitation to "background" gravitational fields. as an example, in some theories with a flat background metric η , gravitational waves follow null geodesics of η , while light follows null geodesics of g . In bran-world scenarios, the apparent speed of gravitational waves could differ from that of light if the former can propagate off the bran into the upper dimensional "bulk". otherwise during which the speed of gravitational waves could differ from c is that if gravitation were propagated by a massive field (a massive graviton), during which case v_g would be given by, in a very local reference frame,

$$\frac{v_g}{c} = \left(1 - \frac{m_g^2 c^4}{E^2}\right)^{1/2} \approx \frac{1}{2} \frac{c^2}{f^2 \lambda_g^2} \quad (2.33)$$

where m_g , E and f are the graviton rest mass, energy and frequency, respectively, and $\lambda_g = h/m_g c$ is the graviton Compton wavelength ($\lambda_g \gg c/f$ assumed). An example of a theory with this property is the two-tensor massive graviton theory of Visser. The most obvious way to test for a massive graviton is to compare the arrival times of a gravitational wave and an electromagnetic wave from the same event, e.g. a supernova. For a source at a distance D , the resulting bound on the difference $|1 - v_g/c|$ or on λ_g is

$$|1 - v_g/c| < 5 \times 10^{-17} km \left(\frac{200 Mpc}{D}\right) \left(\frac{\Delta t}{1s}\right) \quad (2.34)$$

$$\lambda_g > 3 \times 10^{12} km \left(\frac{D}{200 Mpc} \frac{100 Hz}{f}\right)^{1/2} \left(\frac{1}{f \Delta t}\right) \quad (2.35)$$

where $\Delta t \equiv \Delta t_a - (1 + Z)\Delta t_e$ is the "time difference", where Δt_a and Δt_e are the differences in arrival time and emission time, respectively, of the two signals, and Z is the redshift of the source. In many cases, Δt_e is unknown, so that the best one can do is employ an upper bound on Δt_e based on observation or modelling. However, there is a situation in which a bound on the graviton mass can be set using gravitational radiation alone. That is the case of the inspiralling compact binary, the final stage of evolution of systems like the binary pulsar, in which the loss of energy to gravitational waves has brought the binary to an inexorable spiral toward a final merger. Because the frequency of the gravitational radiation sweeps

from low frequency at the initial moment of observation to higher frequency at the final moment, the speed of the gravitational waves emitted will vary, from lower speeds initially to higher speeds (closer to c) at the end. This will cause a distortion of the observed phasing of the waves and result in a shorter than expected overall time Δt of passage of a given number of cycles. Furthermore, through the technique of matched filtering, the parameters of the compact binary can be measured accurately, and thereby the effective emission time Δt_e can be determined accurately. A full noise analysis using proposed noise curves for the advanced LIGO ground-based detectors, and for the proposed space-based LISA antenna yields potentially achievable bounds that are summarized in Table 2.1. These potential bounds can be compared with the solid bound $\lambda_g > 2.8 \times 10^{12}\text{km}$,

Table 2.1: Potentially achievable bounds on λ_g from gravitational-wave observations of in-spiraling compact binaries [25].

$m_1(M_\odot)$	$m_2(M_\odot)$	Distance (Mpc)	Bound on λ_g (km)
Ground-based (LIGO/VIRGO)			
1.4	1.4	300	4.6×10^{12}
10	10	1500	6.0×10^{12}
Space-based (LISA)			
10^7	10^7	3000	$6.9 \cdot 10^{16}$
10^5	10^5	3000	$2.3 \cdot 10^{16}$

derived from solar system dynamics, which limit the presence of a Yukawa modification of Newtonian gravity of the form $V(r) = (GM/r) \exp(-r/\lambda_g)$, and with the model-dependent bound $\lambda_g > 6 \times 10^{19}\text{km}$ from consideration of galactic and cluster dynamics [25].

2.8 The use of gravitational waves to test general relativity

Astronomical sources of gravitational waves are often systems where gravity is extremely strong with relativistic bulk motion of massive objects. The emitted radiation carries the uncorrupted signature of the character of the space-time geometry and thus, it's a useful tool to look at and understand the behavior of matter and geometry under extreme conditions of density, temperature, magnetic fields and relativistic motion [30]. Gravitational waves distort spacetime, in other words they alter the distances between free macroscopic bodies. A gravitational wave passing through the solar system creates a time-varying strain in space that

periodically changes the distances between all bodies within the solar system in a very direction that's perpendicular to the direction of wave propagation [7].

Gravitational waves have access to the foremost extreme gravitational environments in nature. Moreover, gravitational waves travel essentially unimpeded from their source to Earth, and thus, they are doing not suffer from issues related to obscuration. Gravitational waves also exist within the absence of luminous matter, thus allowing us to look at electromagnetically dark objects, like black-hole inspirals [1].

Gravitational waves are most unique in that they propagate without interacting with matter. This permits us to get new information about the universe that electromagnetic waves fail to provide. The amplitude and frequency of gravitational waves describe the frequency and mass of the emitting source. the shape of the ultimate phase of a binary system might give some new insight in astronomy. Stochastic background would reveal the mass distribution of the first plank-scale universe and therefore the evolution of the early universe.

2.9 Gravitational waves detection

The quest to detect gravitational waves is based on our understanding of general relativity (indeed of any theory of gravity that is compatible with special relativity), where the emission of gravitational waves is required by the existence of a fundamental limiting speed for propagation of information. However many of the most interesting sources involve extreme gravity and relativistic speeds, and considerable progress is being made on techniques for solving Einstein's equations to predict confidently the gravitational waves from these sources and to interpret the data taken [30]. The discovery of gravitational waves is imperative for two reasons: to begin with, their location is anticipated to open up a modern window for observational cosmology since the data carried by gravitational waves is exceptionally distinctive from that carried by electromagnetic waves . This new window onto universe will complement our view of the cosmos and will help us unveil the fabric of space-time around black-holes, observe directly the formation of black holes or the merging of binary systems consisting of black holes or neutron stars, search for rapidly spinning neutron stars, dig deep into the very early moments of the origin of the universe, and look at the very center of the galaxies where supermassive black holes weighting

millions of solar masses are hidden. These are only a few of the great scientific discoveries that scientists will witness during the first decade of the 21st century. Second, detecting gravitational waves is important for our understanding of the fundamental laws of physics; the proof that gravitational waves exist will verify a fundamental 85 years old prediction of general relativity. Also, by comparing the arrival times of light and gravitational waves, from, e.g., supernovae, Einstein's prediction that light and gravitational waves travel at the same speed could be checked. [29].

Gravitational waves represent a new phenomenon we can use to understand the universe. The 20th century brought us radio (including microwaves and millimeter waves), x-rays, infrared, and gamma-rays, but all of these tools are electromagnetic phenomena. The 20th century also brought the first promise of non-electromagnetic tools for studying the universe: cosmic ray and neutrino experiments, and finally gravitational waves. Gravitational waves will yield a profound new tool for astronomers. With in gravitational waves we anticipate to identify the increasing speed of mass within the universe, instead of the electromagnetic signature of the mass. For example, we will discriminate between galaxy formation scenarios (Volonteri, Haardt, and Madau 2003), and we can measure the spins of binary black holes directly (Mingarelli et al. 2012; Vitale et al. 2014) [3].

The advanced LIGO detectors at the Livingston and Hanford sites were turned on in September 2015 and the first detection occurred almost immediately there after on 14 September 2015, around 09:50 UTC. The gravitational wave passed through the Livingston detector initially and then through the Hanford detector 7 ms later accounting for the light travel time between the two spatially separated locations. The signal was identified by the online search pipeline merely 3 min after the event. The offline analysis was carried out later confirming the detection and the parameter estimation was performed. The signal to noise ratio was in fact as high as 24 [13].

The observed signal at the output of a detector consists of the true gravitational wave strain h and Gaussian noise. The optimal method to detect a gravitational wave signal leads SNR.

$$\left(\frac{S}{N}\right)_{opt}^2 = 2 \int_0^\infty \frac{|\tilde{h}(f)|^2}{S_n(f)} \quad (2.36)$$

where $\tilde{h}(f)$ is the Fourier transform of the signal waveform and $S_n(f)$ spectral density. It is clear from this expression that the sensitivity of gravitational wave detectors is limited by noise [29].

The peak amplitude of the gravitational wave strain was $h = 10^{-21}$ as can be inferred from Fig.2.7. The band-passed and notched filtered data output from both the detectors is shown within the top two panels of Fig.2.7. The detector output from the two detectors is superimposed after appropriate inversion taking into consideration the light travel time between the two detector locations and also the different orientation of the arms. It matches alright, indicating the presence of the same signal in both the detectors. The signal was generated by the merger of two stellar mass black holes. Masses of the individual black holes were estimated to be $36 M_\odot$ and $29 M_\odot$. In contrast, the mass of the remnant black hole formed as a results of merger was $62 M_\odot$ and it's a dimensionless spin of 0.7. the amount of energy emitted within the gravitational radiation was worth $3 M_\odot$. The distance to the source was 1.3 billion light years. the peak luminosity of the event was 3×10^{56} erg/sec, making it the foremost luminous event exceeding the integrated luminosity of all the celebs taken together within the observable universe. The gravitational signal that's hidden within the noise must be excavated out using optimal data analysis techniques like matched filtering where the expected signal is correlated with the detector output. To this end, a template is used to represent all possible signals from gravitational waves. Therefore, it is very important to obtain an accurate waveform a prior. Within the case of binary black hole coalescence which is that the most promising source of gravitational radiation for ground-based detectors and also the source of the signal detected by LIGO, it's essential to solve two-body problem generally relativity [14]. General relativity describes how two black holes orbiting each other generate gravitational waves, losing energy within the handle, and getting closer together until they merge. We use these predictions of General Relativity to build gravitational waveform models. Whereas there are not yet any waveform models for binary black hole coalescence in other theories of gravity to compare with (they are very difficult to calculate!), we are able still to test the predictions of General Relativity by introducing small modifications to our currently accessible waveform models and compare the data with these "distorted" waveform. Gravitational waves change the relative length of the optical cavities in the interferometer (or equivalently, the proper travel time of photons) resulting in a strain [15]. The word strain is the fractional change in the distance

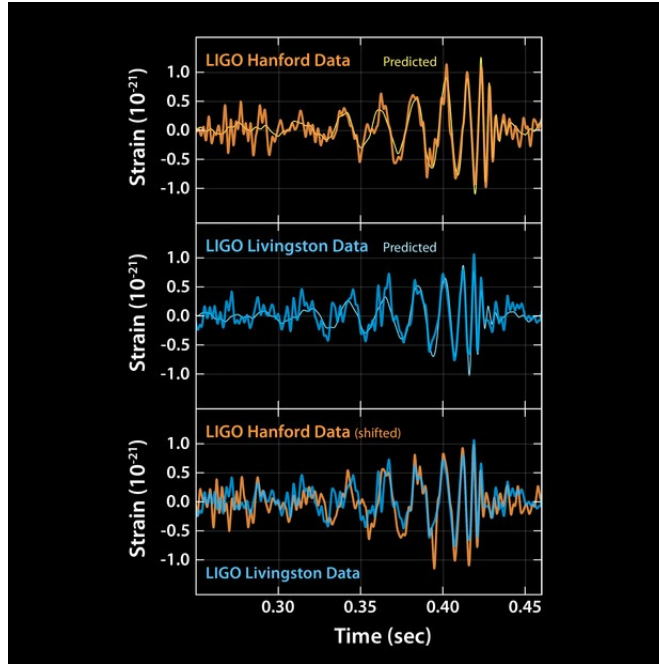


Figure 2.7: The gravitational waveform in this figure correspond to the primary detection event GW150914. The gravitational wave strain is plotted against the clock. the top two panels show the detector output from the LIGO Hanford and LIGO Livingston. The waveform predicted from general theory of relativity are superimposed on the detector output. the underside panel shows the detector output from the LIGO Livingston detector together with that from LIGO Hanford detector shifted appropriately taking under consideration the suspension within the arrival of signal and therefore the difference within the detector orientations. They match well indicating that the identical signal was detected in both the detectors (Image credit: LIGO) [13].

between two measurement points due to the deformation of space-time by a passing gravitational wave.

$$\frac{\Delta L}{L} \quad (2.37)$$

where ΔL is the path length difference between the two arms of the interferometer. Fractional changes is the difference in path lengths along the two arms can be monitored to better than 1 part in 10^{20} . For a simple Michelson interferometer, a difference in path length of order the size of a fringe can easily be detected. For infrared lasers of wavelength $\lambda \sim 1 \mu m$, and interferometer arms of length $L = 4$ km, the minimum detectable strain is

$$h \sim \frac{\lambda}{L} \sim 3 \times 10^{-10}. \quad (2.38)$$

This is far from 10^{-20} . However, changes in the length of the cavities corresponding to fractions of a single fringe can also be measured provided we have a sensitive

photodiode at the dark port of the interferometer, and enough photons to perform the measurement. This way we can track changes in the amount of light incident on the photodiode as the lengths of the arms change and we move over a fringe. The rate at which photons arrive at the photodiode is a Poisson process and the fluctuations in the number of photons is $\sim N^{1/2}$, where N is the number of photons. Therefore we can track changes in the path length difference of order

$$\Delta L \sim \frac{\lambda}{N^{1/2}}. \quad (2.39)$$

The number of photons depends on the laser power P , and the amount of time available to perform the measurement. For a gravitational wave of frequency f , we can collect photons for a time $t \sim \frac{1}{f}$, so the number of photons is

$$N \sim \frac{P}{fh_p\nu} \quad (2.40)$$

where h_p is Planck's constant and $\nu = c/\lambda$ is the laser frequency. For a typical laser power $P \sim 1W$, a gravitational-wave frequency $f = 100$ Hz, and $\lambda \sim 1 \mu m$ therefore, the number of photons is $N \sim 10^{16}$. So that the strain we are sensitive to becomes

$$h \sim 10^{-18}. \quad (2.41)$$

The sensitivity may be further improved by increasing the effective length of the arms. within the LIGO instruments, for instance, each of the two arms forms a resonant Fabry–Pérot cavity. For gravitational-wave frequencies smaller than the inverse of the light storage time, the light within the cavities makes many back and forth trips in the arms, while the wave is traversing the instrument. For gravitational waves of frequencies around 100 Hz and below, the light makes a few thousand back and forth trips while the gravitational wave is traversing the interferometer, which ends in a very three orders of magnitude improvement in sensitivity,

$$h \sim 10^{-21}. \quad (2.42)$$

For frequencies larger than 100 Hz the number of round trips the light makes in the Fabry-Pérot cavities while the gravitational wave is traversing the instrument is reduced and the sensitivity is degraded [1].

2.10 Summary

In 1915, GR is published by Albert Einstein as the geometrical theory of gravitation. GR is distinguished from other metric theories of gravitation by its use of the

Einstein field equations to relate spacetime content and spacetime curvature. GR is currently the most successful gravitational theory, being almost universally accepted and well confirmed by observations. Einstein's theory of general relativity, the geometry of space-time is a dynamic physical observable that supports wave-like excitation, propagating at the speed of light. These are known as gravitational waves. GWs are disturbances in the curvature of space-time, generated by accelerated masses, that propagate as waves outward from their source at the speed of light. Like all sorts of waves, gravitational waves carry the energy and in fact transport, it away from the source. GW propagates with out interacting with matter, this provides to get modern information about the evolution the early univers and used to observe and understand the behavior of matter and geometry under extreme conditions of density, temperature, magnetic fields, and relativistic motion.

Methods of analyzing gravitational waves to verify Einstein general theory of relativity in binary black hole and its waveform models

3.1 Introduction

In order to study GR from the gravitational waves radiated by the binary black hole we have used different GW models including, the quadrupole formalism as an approximation of general relativity in the two-body problem, effective-one-body and phenomenological waveform model, and also numerical relativity simulated waveforms. In this chapter, we will briefly recall how the gravitational waves are derived from the Einstein field equations and under which conditions it work. In a weak gravitational field, i.e. for a nearly flat space-time, we can simplify the Einstein equations. The goal is to show that $h_{\mu\nu}$ obeys wave equations.

3.2 Einstein field equation

The fundamental equation that relates the spacetime metric (i.e., the gravitational field) to the distribution of energy is Einstein's field equation [9]. Let us begin by recalling the field equation of Newtonian gravity

$$\vec{\nabla}^2 \Phi = 4\pi G \rho \quad (3.1)$$

If gravity is a manifestation of spacetime curvature that is for a weak gravitational field, in coordinates such that $g_{\mu\nu} = \eta_{\mu\nu} + h_{\mu\nu}$ (with $|h_{\mu\nu}| \ll 1$), each element of $g_{\mu\nu}$ is close to its inertial value. Non-relativistic motion, on the other hand, implies that $\tau \approx t$, $\frac{dx^0}{d\tau} \approx c$, $\frac{dx^i}{d\tau} \approx v^i \ll c$ so the geodesic Equation

$$\ddot{x}_\rho + \Gamma_{k\lambda}^\rho \dot{x}^k \dot{x}^\lambda = 0 \quad (3.2)$$

with $\rho = i$ becomes

$$\frac{1}{c^2} \frac{d^2 x^i}{dt^2} + \Gamma_{00}^i = 0 \quad (3.3)$$

since the terms in $\frac{dx^i}{d\tau}$ are neglected. We may write this equation as

$$\frac{d^2x^i}{d\tau^2} = a^i - c^2\Gamma_{00}^i \quad (3.4)$$

then the right hand side represents the ‘gravitational force’, which gives the particle its acceleration. The connection coefficient in Eq.3.3 is

$$\Gamma_{00}^i = \frac{1}{2}g^{i\sigma}(2g_{0\sigma,0} - g_{00,\sigma}) = -\frac{1}{2}g^{ik}g_{00,0}\Gamma_{00}^i \approx -\frac{1}{2}\eta^{ik}\frac{\partial h_{00}}{\partial x^k} = -\frac{1}{2}\nabla_i h_{00} \quad (3.5)$$

noting that η is constant, but keeping only first order terms in η , and the final equality since $\eta^{ik} = \delta^{ik}$ for spacelike indices. Putting Eq.3.5 into Eq.3.3 gives

$$\frac{d^2x^i}{dt^2} = \frac{c^2}{2}\nabla_i h_{00} \quad (3.6)$$

This is to be compared with Newton’s equation

$$\frac{d^2\mathbf{x}}{dt^2} = \mathbf{g} = -\nabla\phi \quad (3.7)$$

Where ϕ is the gravitational potential. Comparison of Eq.3.6 and Eq.3.7 give[8]

$$h_{00} = -\frac{2\phi}{c^2} \quad (3.8)$$

and hence

$$g_{00} = -\left(1 + \frac{2\Phi}{c^2}\right) \quad (3.9)$$

The correct relativistic description of matter is provided by the energy-momentum tensor and, for a perfect fluid or dust, in the inertial reference frame(IRF) we have

$$T_{00} = \rho c^2. \quad (3.10)$$

For a weak static gravitational field in the low-velocity limit,

$$\vec{\nabla}^2 g_{00} = \frac{8\pi G}{c^4} T_{00} \quad (3.11)$$

Einstein’s fundamental intuition was that the curvature of spacetime at any event is related to The above considerations thus suggest that the gravitational field equations should be of the form

$$K_{\mu\nu} = kT_{\mu\nu} \quad (3.12)$$

where $K_{\mu\nu}$ is a rank-2 tensor related to the curvature of spacetime and we have set $k = 8\pi G/c^4$. Since the curvature of spacetime is expressed by the curvature tensor $R_{\mu\nu\sigma\rho}$, the tensor $K_{\mu\nu}$ must be constructed from $R_{\mu\nu\sigma\rho}$ and the metric tensor $g_{\mu\nu}$. Moreover, $K_{\mu\nu}$ should have the following properties:

- i. The Newtonian limit suggests that $K_{\mu\nu}$ should contain terms no higher than linear in the second-order derivatives of the metric tensor; and
- ii. Since $T_{\mu\nu}$ is symmetric then $K_{\mu\nu}$ should also be symmetric. The curvature tensor $R_{\mu\nu\sigma\rho}$ is already linear in the second derivatives of the metric, and so the most general form for $K_{\mu\nu}$ that satisfies (i) and (ii) is

$$K_{\mu\nu} = aR_{\mu\nu} + bRg_{\mu\nu} + \lambda g_{\mu\nu} \quad (3.13)$$

where $R_{\mu\nu}$ is the Ricci tensor, R is the curvature scalar and a, b, λ are constants. Let us now consider the constants a, b, λ . First, if we require that every term in $K_{\mu\nu}$ is linear in the second derivatives of $g_{\mu\nu}$ then we see immediately that $\lambda = 0$. We will relax this condition later, but for the moment we therefore have

$$K_{\mu\nu} = aR_{\mu\nu} + bRg_{\mu\nu} \quad (3.14)$$

To find the constants a and b we recall that the energy-momentum tensor satisfies $\nabla_{\mu}T_{\mu\nu} = 0$;

$$\nabla K_{\mu\nu} = \nabla(aR^{\mu\nu} + bRg^{\mu\nu}) \quad (3.15)$$

However, $\nabla(R^{\mu\nu} - \frac{1}{2}Rg^{\mu\nu}) = 0$ and $\nabla_{\mu}g_{\mu\nu} = 0$, We obtain

$$\nabla_{\mu}K^{\mu\nu} = (\frac{1}{2}a + b)g^{\mu\nu}\nabla_{\mu}R = 0 \quad (3.16)$$

The quantity $\nabla_{\mu}R$ will, in general, be non-zero through out (a region of) spacetime unless the latter is flat and hence there is no gravitational field. Thus we find that $b = -a/2$, and so the gravitational field equations must take the form

$$a \left(R_{\mu\nu} - \frac{1}{2}g_{\mu\nu}R \right) = kT_{\mu\nu} \quad (3.17)$$

Comparing the weak-field limit of these equations with Poisson's equation in Newtonian gravity and putting $a = 1$ and so [31].

$$R_{\mu\nu} - \frac{1}{2}g_{\mu\nu}R = kT_{\mu\nu} \quad (3.18)$$

where $k = 8\pi G/c^4$. Eq.3.18 constitutes Einsteins gravitational field equations, which form the mathematical basis of the theory of general relativity. We note that the left-hand side of Eq.3.18 is simply the Einstein tensor $G_{\mu\nu}$,

$$G_{\mu\nu} = \frac{8\pi G}{c^4}T_{\mu\nu} \quad (3.19)$$

3.2.1 Einstein equations in empty space

A region of spacetime in which $T_{\mu\nu} = 0$ is called empty, and such a region is therefore not only devoid of matter but also of radiative energy and momentum. The gravitational field equations for empty space are

$$R_{\mu\nu} = 0 \quad (3.20)$$

In the weak-field approximation, spacetime is only 'slightly' curved and so there exist coordinates in which $g_{\mu\nu} = \eta_{\mu\nu} + h_{\mu\nu}$ (with $|h_{\mu\nu}| \ll 1$), and the metric is stationary [31].

where $\eta_{\mu\nu}$ is the flat metric expressed in cartesian coordinates and $h_{\mu\nu}$ is the tiny perturbation around it and the vacuum Einstein equations are linearised in $h_{\mu\nu}$, we get the wave equation $\square h_{\mu\nu} = 0$ [13].

$$\eta_{\mu\nu} = \begin{pmatrix} c^2 & 0 & 0 & 0 \\ 0 & -1 & 0 & 0 \\ 0 & 0 & -1 & 0 \\ 0 & 0 & 0 & -1 \end{pmatrix} \quad (3.21)$$

Ignoring all terms that are non linear in h the Christoffel symbols become

$$\begin{aligned} \Gamma_{\mu\nu}^{\rho} &= \frac{1}{2}g^{\rho\sigma}(\partial_{\mu}g_{\nu\sigma} + \partial_{\nu}g_{\mu\sigma} - \partial_{\sigma}g_{\mu\nu}) \\ &= \frac{1}{2}\eta^{\rho\sigma}(\partial_{\mu}h_{\nu\sigma} + \partial_{\nu}h_{\mu\sigma} - \partial_{\sigma}h_{\mu\nu}) \end{aligned} \quad (3.22)$$

The Ricci curvature tensor becomes

$$\begin{aligned} R_{\mu\nu} &= \partial_{\mu}\Gamma_{\nu\rho}^{\rho} - \partial_{\rho}\Gamma_{\mu\nu}^{\rho} + \Gamma_{\mu\rho}^{\sigma}\Gamma_{\sigma\nu}^{\rho} - \Gamma_{\mu\nu}^{\sigma}\Gamma_{\sigma\rho}^{\rho} \\ R_{\mu\nu} &= \partial_{\mu}\Gamma_{\nu\rho}^{\rho} - \partial_{\rho}\Gamma_{\mu\nu}^{\rho} \end{aligned} \quad (3.23)$$

$$\begin{aligned} R_{\mu\nu} &= \frac{1}{2}\eta^{\rho\sigma}(\partial_{\mu}\partial_{\rho}h_{\nu\sigma} + \partial_{\mu}\partial_{\nu}h_{\rho\sigma} - \partial_{\mu}\partial_{\sigma}h_{\rho\nu}) - \frac{1}{2}\eta^{\rho\sigma}(\partial_{\rho}\partial_{\mu}h_{\nu\sigma} + \partial_{\rho}\partial_{\nu}h_{\mu\sigma} - \partial_{\rho}\partial_{\sigma}h_{\mu\nu}) \\ &= \frac{1}{2}\eta^{\rho\sigma}(\partial_{\mu}\partial_{\nu}h_{\rho\sigma} - \partial_{\mu}\partial_{\sigma}h_{\rho\nu} - \partial_{\rho}\partial_{\nu}h_{\mu\sigma} + \partial_{\rho}\partial_{\sigma}h_{\mu\nu}) \end{aligned} \quad (3.24)$$

The scalar curvature becomes

$$\begin{aligned} R &= R_{\mu\nu}g^{\mu\nu} = \frac{1}{2}\eta^{\mu\nu}\eta^{\rho\sigma}(\partial_{\mu}\partial_{\nu}h_{\rho\sigma} - \partial_{\mu}\partial_{\sigma}h_{\rho\nu} - \partial_{\rho}\partial_{\nu}h_{\mu\sigma} + \partial_{\rho}\partial_{\sigma}h_{\mu\nu}) \\ &= \frac{1}{2}\eta^{\mu\nu}\eta^{\rho\sigma}(\partial_{\mu}\partial_{\nu}h_{\rho\sigma} - \partial_{\mu}\partial_{\sigma}h_{\rho\nu}) \end{aligned} \quad (3.25)$$

Now, imposing the harmonic coordinat condition:

$$\partial_{\gamma}h_{\alpha\beta}\eta^{\beta\gamma} = \frac{1}{2}\partial_{\alpha}h_{\beta\gamma}\eta^{\beta\gamma} \quad (3.26)$$

The Ricci tensor and curvature scalar becomes

$$R_{\mu\nu} = \eta^{\rho\sigma} (\partial_\mu \partial_\nu h_{\rho\sigma} - \partial_\mu \partial_\sigma h_{\rho\nu} - \partial_\rho \partial_\nu h_{\mu\sigma} + \partial_\rho \partial_\sigma h_{\mu\nu})$$

$$R_{\mu\nu} = \eta^{\rho\sigma} (\partial_\mu \partial_\nu h_{\rho\sigma} - \frac{1}{2} \partial_\mu \partial_\nu h_{\rho\sigma} - \frac{1}{2} \partial_\mu \partial_\nu h_{\rho\sigma} + \partial_\rho \partial_\sigma h_{\mu\nu}) = \frac{1}{2} \square h_{\mu\nu} \quad (3.27)$$

$$R = \eta^{\mu\nu} \eta^{\rho\sigma} (\partial_\mu \partial_\nu h_{\rho\sigma} - \partial_\mu \partial_\sigma h_{\rho\nu}) = \eta^{\mu\nu} \eta^{\rho\sigma} (\frac{1}{2} \partial_\mu \partial_\rho h_{\nu\sigma} - \frac{1}{2} \partial_\mu \partial_\rho h_{\sigma\nu}) = 0 \quad (3.28)$$

Now, inserting all of this into Einstein field equation

$$R_{\mu\nu} - \frac{1}{2} R g_{\mu\nu} + \Lambda g_{\mu\nu} = \frac{8\pi G}{c^4} T_{\mu\nu}. \quad (3.29)$$

So the Einstein field equation in vacuum gives

$$\frac{1}{2} \square h_{\mu\nu} = \frac{8\pi G}{c^4} T_{\mu\nu} - \Lambda (\eta_{\mu\nu} + h_{\mu\nu}) \quad (3.30)$$

without cosmological constant

$$\square h_{\mu\nu} = \frac{16\pi G}{c^4} T_{\mu\nu} \quad (3.31)$$

In the vacuum:

$$\square h_{\mu\nu} = 0 \quad (3.32)$$

Here \square is the flat space *d'Alembertian*.

$$\square = \partial^\lambda \partial_\lambda = g^{\mu\nu} \partial_\nu \partial_\mu = \frac{1}{c^2} \frac{\partial^2}{\partial t^2} - \frac{\partial^2}{\partial x^2} - \frac{\partial^2}{\partial y^2} - \frac{\partial^2}{\partial z^2} \quad (3.33)$$

$$\square = \frac{1}{c^2} \frac{\partial^2}{\partial t^2} - \nabla^2 \quad (3.34)$$

wher ∇^2 is 3-dimensional laplacian. Thus, it implies that the metric perturbation $h_{\mu\nu}$ represents the wave that travels at the speed of light and it is known as the gravitational wave [13].

3.2.2 Linear approximation of Einstein field equations

Along with the tests for GR, it is important to test the behavior of the resulting gravitational waves. As described in this section the analysis of GWs is based on approximation theories and fundamental assumptions. Hence, it is important that we test this approach for its consistency with GR. Gravitational waves can be described using linear approximation of gravity. This makes it conceivable to use the weak-field metric to discover arrangements to the Einstein equation in a space-time with a geometry close to flat space-time. In general relativity gravitational waves are most easily described when propagating in nearly flat space-time, that is, in nearly empty space. Gravitational waves far from their source are small

ripples in space-time and cause small curvatures in the otherwise flat geometry. In this valid for weak estimation, terms non linear in h are ignored, and indices are raised and brought down with Min Kowski metric. The gravitational wave curvature tensor h can be considered as the gravitational wave field. The wave field is transverse and trackless, and for waves traveling in the z -direction may be expressed as follows:

$$h_{\mu\nu} = \begin{bmatrix} 0 & 0 & 0 & 0 \\ 0 & h_{xx} & h_{xy} & 0 \\ 0 & h_{yx} & h_{yy} & 0 \\ 0 & 0 & 0 & 0 \end{bmatrix} \quad (3.35)$$

There is no z -component due to the transverse nature of the waves, and to be traceless h satisfies

$$h_{xx} = -h_{yy}. \quad (3.36)$$

Because the Riemann tensor is symmetric, h also satisfies

$$h_{xy} = h_{yx}. \quad (3.37)$$

The symmetry of h means that there are just two possible independent polarization states which are usually denoted h_+ and h_\times . In the case of sinusoidal gravitational waves we can express these polarizations as

$$h_+ = h_{xx} = \text{Re}[A_+ e^{-i\omega(t-z/c)}] \quad (3.38)$$

$$h_\times = h_{xy} = \text{Re}[A_\times e^{-i\omega(t-z/c)}] \quad (3.39)$$

Here A_+ and A_\times are the strain amplitudes of each polarization.

3.2.3 Quadrupole formalism

The simplest technique for computing the gravitational wave field within the presence of matter is that the quadrupole formalism. Einstein himself derived the quadrupole formula for gravitational radiation by solving the linearized equations. This formalism is specially important because it's very accurate for several astrophysical sources of gravitational waves and is simple to calculate. It doesn't require for prime accuracy in the computation on the strength of the source's internal gravity, but requires that internal motions inside the source are slow compared to the speed of light. This requirement implies that the wavelength of the gravitational waves emitted is much larger than the source's characteristic size, $\lambda \gg L_s$. The lowest allowed multi pole for gravitational radiation is that the quadrupole. The mono pole is

forbidden as a results of mass conservation. in a similar way, dipole radiation is absent as a results of momentum conservation. The quadrupole formalism allow us to urge an expression for the gravitational wave field:

$$h_{ij}(t, x^i) = \frac{2}{R} \frac{G}{c^4} \ddot{Q}_{ij}^{TT} \left(t - \frac{R}{c} \right) \quad (3.40)$$

where R is the euclidean distance from the point x^i to the center of the source and t is the proper time measured by the observer. The quantity Q_{ij} is the symmetric part of the second moment of the sources mass density ρ computed in a cartesian coordinate system centered on the source evaluated at the retarded time $t_{ret} = t - \frac{R}{c}$

$$Q_{ij}^{TT} = \int d^3x \rho (x_i x_j - \frac{1}{3} \delta_{ij} r^2) \quad (3.41)$$

The superscript TT means that one needs to keep only the part that is transverse to the direction of propagation of the wave and is traceless [11].

3.2.4 Two-body problem

As a primary application of numerical relativity, we consider the gravitational two- body problem. The two-body problem in Newtonian gravitational physics is formulated for two point masses moving in their mutual gravitational field. A particular solution of the Newtonian two-body problem could be a Keplerian elliptical orbit. However, in Einsteinian gravity, such orbital rotation generates gravitational waves that take away energy and momentum. Binary orbits therefore decay, band the motion of the two bodies follows an inward spiral that eventually terminates with the collision and merger of the two objects. In most astrophysical situations, the energy loss because of the emission of gravitational waves is so small that a binary orbit decays only on time scales of millions or billions of years. However, for compact objects like, neutron stars or black holes in very tight binaries, general relativistic effects like, gravitational wave emission play a serious role [5].

One of the foremost important applications of the quadrupole formalism as an approximation to general relativity theory is that the two-body problem, i.e. the matter of finding the motion and gravitational radiation of self gravitating relativistic systems of two extended bodies. This calculation relies on a Newtonian description of the dynamics of the two bodies. The Newtonian dynamics will depart from the relativistic description when the relative velocity of the binary is comparable the speed of light or when the gravitational energy becomes large compared to the rest

mass energy of the system. Relativistic binary systems exist within the universe, samples of this are neutron stars or black holes binaries. These systems emit gravitational waves and are the most prominent sources of gravitational radiation that may be detected by LIGO. Surprisingly one can learn lots from the collision of two bodies using the quadrupole formalism presented above. A Newtonian positional notation is illustrated in Fig.3.1. For simplicity allow us to assume that the system follow circular orbits and therefore the masses are equal. Thus

$$M_1 = M_2 = M, \quad \text{and} \quad R_1 = R_2 = R. \quad (3.42)$$

Introducing cylindrical coordinates

$$x(t) = R \cos \Omega t, \quad y(t) = R \sin \Omega t, \quad z(t) = 0. \quad (3.43)$$

The nonzero components of the quadrupole moment are

$$Q_{xx} = \frac{MR^2}{2} \left(\frac{1}{3} + \cos 2\Omega t \right), \quad Q_{yy} = MR^2 \left(\frac{1}{3} - \sin 2\Omega t \right), \quad Q_{zz} = -\frac{2}{3}MR^2 \quad (3.44)$$

Taking the third time derivative and replacing into the expression to compute the

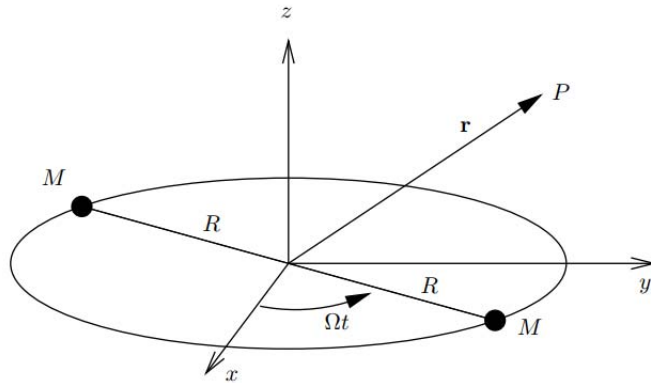


Figure 3.1: Two bodies with equal masses orbiting around their center of mass in circular orbits [11].

gravitational source wave luminosity as the energy lost by the source

$$L_{gw} = -\frac{dE^{source}}{dt} \quad (3.45)$$

$$L_{gw} = \frac{G}{5c^5} \langle \ddot{Q}^{ij} \ddot{Q}_{ij} \rangle \quad (3.46)$$

$$L_{gw} = \frac{G}{5c^5} \langle (\ddot{Q}_{xx})^2 + (\ddot{Q}_{xy})^2 + (\ddot{Q}_{yy})^2 + (\ddot{Q}_{zz})^2 \rangle \quad (3.47)$$

$$= \frac{32G}{5c^5} \Omega^6 M^2 R^4 \quad (3.48)$$

The angular frequency Ω and the period T are related by $\Omega = 2\pi/T$. Furthermore, using Kepler's third law: $R^3 = \frac{GMT^2}{4\pi^2}$ the gravitational wave luminosity can be expressed in terms of T

$$L_{GW} = \frac{32}{5} 2^{10/3} \frac{c^5}{G} \left(\frac{\pi GM}{c^3 T} \right)^{10/3} \quad (3.49)$$

This may be an enormous luminosity for example, the estimated luminosity for the event GW150914 is $L \sim 0.2 \times 10^{-3} L_0$, where the Planck luminosity is $L_0 := c^5/G \sim 10^{59} \text{erg/s}$. By comparison, the luminosity of the sun is $L_\odot = 3.839 \times 10^{33} \text{erg/s}$. The Newtonian binding energy of the binary is $E = -\frac{1}{2} \frac{GmM}{R}$, and taking the derivative

$$\frac{dE}{dt} = \frac{GmM}{2R^2} \frac{dR}{dt} \quad (3.50)$$

Thus as the gravitating system losses energy by emitting radiation, the distance between the two bodies decreases at a rate

$$\frac{dR}{dt} = \frac{64 G^3 M^3}{5 c^5 R^3} \quad (3.51)$$

The size of the binary orbit decreases and the components move faster leading to emission of gravitational waves with increasing amplitude and frequency. This last stage is known as the *chirp* signal.

The orbital frequency increases accordingly to.

$$\frac{1}{T} \frac{dT}{dt} = \frac{3}{2} \frac{1}{R} \frac{dR}{dt}, \quad (3.52)$$

and the system will merge after a time t_{merger}

$$t_{\text{merger}} = \frac{5}{256} \frac{c^5}{G^3} \frac{R_0^4}{M^5} \quad (3.53)$$

where R_0 is the initial separation. The previous analysis can be generalized to consider elliptic orbits, but it is possible to shown that gravitational wave emission circularize the orbits faster than the coalescence time-scale, making the study of circular orbits quite useful [11].

3.3 Numerical relativity

Numerical relativity is that the science of numerically simulating the predictions of the speculation of Einstein's general theory of relativity on a supercomputer.

This includes modeling the mergers of binaries containing black holes and neutron stars, accretion disks within the ultra relativistic regime, and stellar collapse, among others. Solving the complete Einstein equations on the computer is that the subject of numerical relativity, which could also be called computational general theory of relativity. Numerical relativity spans a large range of different topics

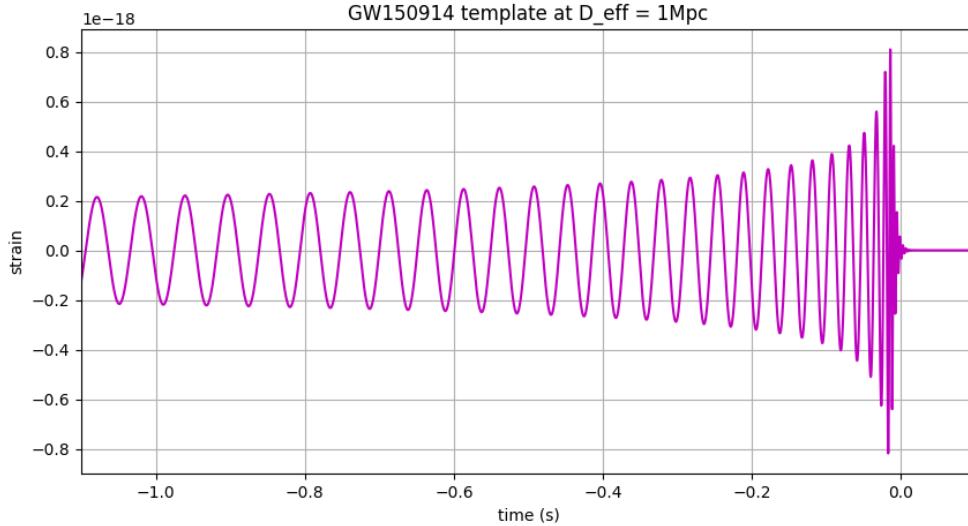


Figure 3.2: Numerical waveform template.

including numerical methods for partial differential equations, astrophysics, mathematical general relativity, computer programming, and simulation science. Current research in numerical relativity is in a transition from a self-contained topic in theoretical physics to a physical theory with numerous connections to observational astronomy. NR is providing key theoretical predictions and analysis tools for the ongoing gravitational wave observations. As shown in Fig.2.4 gravitational waveform can be extracted by various methods in different phases of the binaries. In-spiral phase waveform can be extracted by post-Newtonian approximation, merger by numerical relativity and finally ring- down by perturbation theory [32]. Any BBH signal, whether generated using numerical relativity or observed in the strain data at a LIGO detector, can be written in the frequency domain as

$$\bar{h}_{GR}(f) = A(f)e^{i\phi(f)} \quad (3.54)$$

where $A(f)$ represents the amplitude of the waveform and $e^{i\phi(f)}$ represents the complex phase [33].

One of the foremost important promises of GW astronomy is to test GR within the

highly dynamical, strong field regime. BBHs are prime candidates for this, as the gravitational fields are extreme and therefore the BH speeds are relativistic as one approaches the merger. Tests of GR typically place the foremost stringent accuracy requirements on waveform models, as systematic biases in waveform models could lead to a bias being misidentified as a violation of GR. Therefore, to maximize the science output of our detectors and to meet the promise of GW astronomy, it is vital to possess an accurate waveform model. As mentioned in Fig.2.4 perturbation schemes like PN break down as one approaches the merger of a BBH, and NR is the only method which will accurately predict the end result. NR simulations are very accurate, being limited mainly by the resolution of the grid used. However, these simulations are prohibitively expensive for many direct data analysis applications, with each simulation taking a few month on a supercomputer. Therefore, several approximate waveform models are developed over the years. the two main approaches are dubbed "phenomenological" and "effective-one-body" waveform. These models typically make some assumptions about the phenomenology of the waveform, supported good physical motivations. Then, any remaining free parameters are set by calibrating against NR simulations. These models also are quite fast and are utilized in analyzing the signals seen by LIGO/Virgo. While these models are shown to be accurate enough for current detector sensitivities, they typically have a lower accuracy than NR simulations [14].

3.4 Effective one body formalism

The Effective-One-Body (EOB) method is a resourceful formalism developed by Damour and Buonanno in 1999. during this framework, the two-body problem is reformulated and described jointly effective body on an efficient metric, whose dynamics is described by an effective Hamiltonian. This framework heavily uses post-Newtonian results along with re-summation techniques consisting of re-writing in an exceedingly factorized form the post-Newtonian development used. The effective-one-body method also uses numerical relativity results to inform and adjust certain parameters, especially during the merger and therefore the ring-down phases[24]. Several recent comparisons between EOB predictions and Numerical Relativity simulations have shown the aptitude of the EOB formalism to produce accurate descriptions of the dynamics and radiation of varied binary systems (comprising black holes or neutron stars) in regimes that are inaccessible to other analytical approaches (such as the last orbits and therefore the merger of comparable mass

black holes). The EOB formalism is probably going to produce an efficient way of computing the very many accurate template waveform that are needed for Gravitational Wave (GW) data analysis purposes.

3.5 IMRPhenom

The second family of templates used are phenomenological templates usually called IMRPhenom templates (IMR standing for In-spiral-Merger-Ringdown). These templates are built in the Fourier space and parametrize the signal with a collection of coefficients that are determined either using post-Newtonian results (for the in-spiral), black hole perturbation (for the ring-down) or by calibration to numerical relativity (for the merger). Besides, they contain extra coefficients accustomed describe phenomenologically the intermediate phase between the inspiral and the merger [24]. For consistency with the labeling used within the LIGO-Virgo Collaboration refers to the present model as "IMRPhenomA" refers to a model of non-spinning binaries, and "IMRPhenomB" to an earlier model of non-processing binaries, "IMRPhenomC" it incorporates higher-order PN information within the in-spiral phasing, but also make cross-checks against the IMRPhenomB model [34].

3.6 Summary

In this chapter we have described modes for all the quantities that are necessary to accomplish our objectives. We have derive the GW by Linear approximation of Einstein field equations and also we have presented all the waveform models necessary to compute the GW data analysis process and the GR are computed using NR simulation. Numerical relativity is providing key theoretical predictions and analysis tools for the ongoing gravitational wave observations.

Result And Discussion

4.1 Introduction

In GR, when two BHs merge, they form a highly distorted BH, that then rings down to settle to a final Kerr state. The GWs radiated as the distorted BH settles down is known as the post-merger signal in a BBH waveform. Qualitatively, the post-merger signal contains two phases. The early part of the post-merger signal carries information about the highly non-linear dynamics of the strong field region (close to the BH). This part of the signal can only be modelled by solving the full Einstein's equation using NR. As the BH evolves towards its final state, the non-linearity is dissipated as GW and eventually, the system can be modelled as a linear perturbation on the spacetime of the final Kerr BH [35]. In this chapter we will see the GW signals given by different models and also we prove or disprove whether GR pass the test of GW, this can be done by comparing LIGO to the EOBNR and phenomenological wave form models and also comparing to solution of GR simulated by NR.

4.1.1 Plus and cross polarization of gravitational waves

So far, it has been said that the gravitational wave have two polarization, the gravitational waves was detected by the LIGO, which assist underpins GR. To affirm that GR is the hypothesis of gravity, the polarization of GWs need to be decided. It is well known that there are two polarization in GR, the plus, and the cross. We can see that these polarization contrast by the stage of the signals. This holds for system where the orbital plane of the binary doesn't process. Within the zoom-in plot(right-hand side of Fig.4.1), ready to see the merger itself and the ring-down that takes after. It can be interesting to plot both polarization on the same plot in order to have a view of their difference. It can be seen that the two polarization have a slight shift between them. Therefore, using one or the other

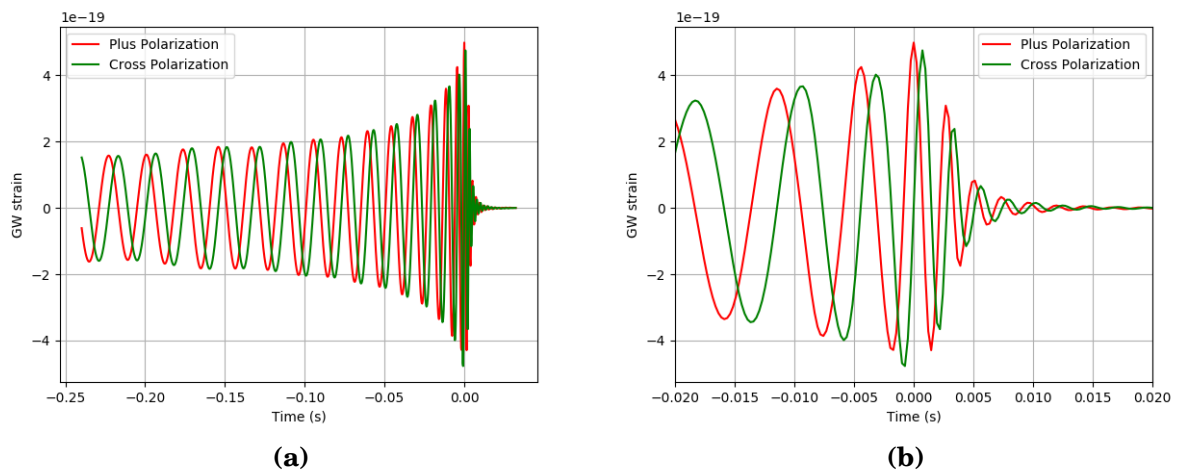


Figure 4.1: Waveform for the IMRPhenomB model of both polarization after inverse Fourier transform, the figure constructed from two equal $20M_{\odot}$ of black hole with lower frequency of $40Hz$, the right one is zoomed around the time of the merger. We have a better view on the ring down part, where the amplitude decreases to zero. A shift can be observed between the two polarization.

can make a slight difference in the timing of events. In addition, when carefully looked at the figure, it shows that the amplitude is not totally the same. Indeed, the maximum of the cross polarization is slightly higher than that of the plus polarization. It can also be noted that the cross polarization becomes flat a bit later than the plus polarization in time. So, one sees that both polarization are important for the analysis as they are not the same. The difference comes from the phase of the signal. This is true as long as the orbital plane of the binary system is not processing. Since GR is the source of the gravitational wave, subsequently, the gravitational wave gives a modern strategy to examine GR and its alternatives within the high speed, strong-field regime. We drive gravitational wave equation by linear approximation of Einstein field equations and the solution of this equation is wave-like as shown in Fig.4.1, so that from this solition we are able to verify that GR passes the test of a gravitational wave.

4.1.2 Power spectral density

Power spectral density can be built for each detector based on the data sample. It is a way to represent the sensitivity of the detector as it gives the square of the strain that the noise produces for each frequency. This spectrogram shows how the PSD of the data changes over time. The most highlight we see is that the low frequencies contain more power than the high frequencies. In both detectors, we can see that

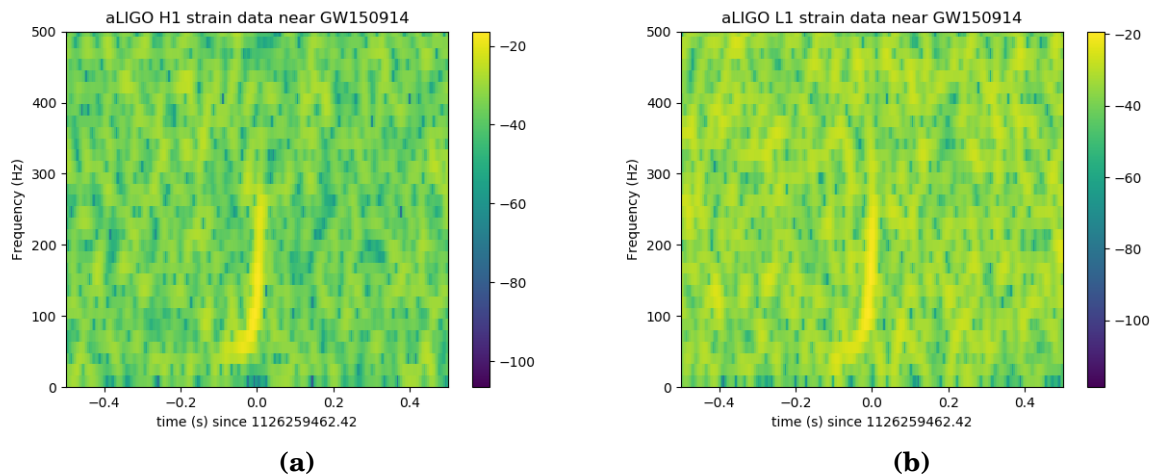
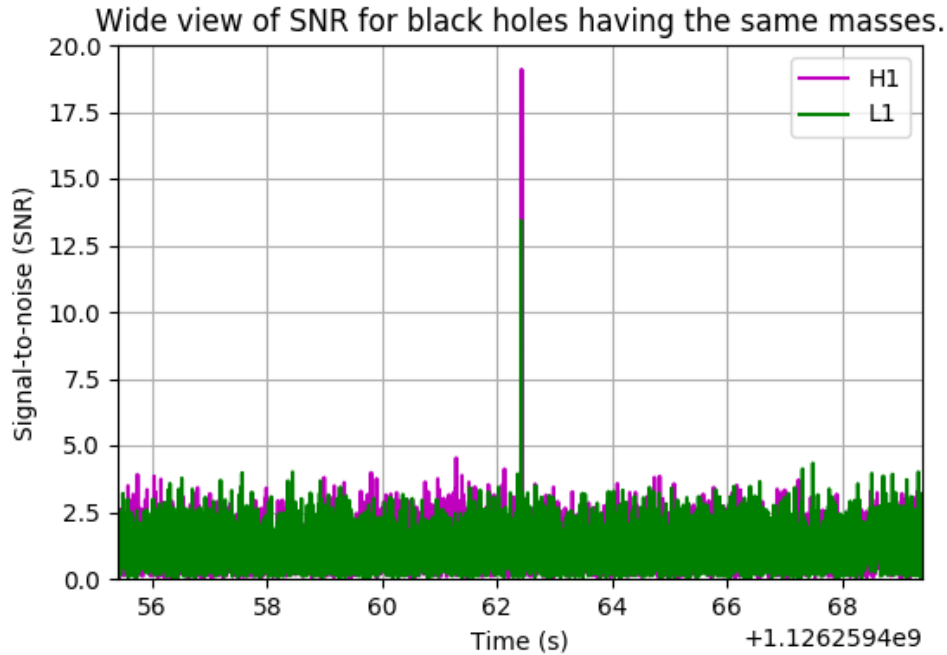


Figure 4.2: zoomed and whitening data over the range of 20 Hz to 400 Hz around the event time = 1126259462.422 se. The left panel shows the Hanford data and the right panel shows the Livingston data at the time of GW150914.

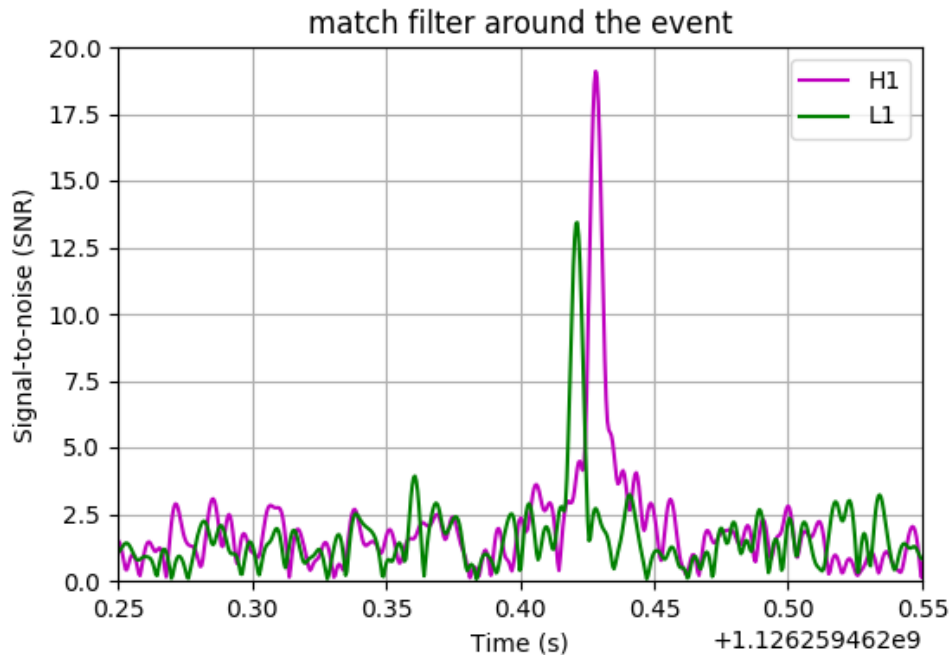
similar GW signals chirping from lower to higher frequency over a small fraction of second in the frequency range of 20 Hz to 400 Hz. But a more visible signal is seen between 20 Hz and 300 Hz. This high signal region is the merger of the binary black hole. More clear signal is seen from Hanford detector than the Livingston detector therefore, the Hanford detector is more powerful (sensitive) than the Livingston detector.

4.1.3 Signal to noise ratio

Since signal-to-noise ratio is a measure of whether a particular signal has been detected at a statistically significant level. Low values of SNR mean that a signal has not been detected, while very high values imply a nearly certain detection. So, from Fig.4.3 we can examine maximum value of gravitational wave signal, this region is the merger of the binary black holes as the two systems closer to each other the amplitude of the gravitational wave signal increase because the mass of the binary increase as the binary black hole closer to each other, this time the binary radiates high energy in the form of gravitational wave, while during ring down phase the binary changed to single remnant black hole therefore the final black hole mass is less than the total mass of the binary ($m_f < m_{tot}$). Fig.4.3 gives a more detailed picture of the SNR in the detectors around the time of the event. One clearly sees the presence of two peaks in the signal with a time delay between them corresponding to the time needed for the wave to travel from one detector to the other, from the second figure we see that the gravitational wave is first detected



(a) Wide view of the SNR for the template with black holes having the same masses.



(b) Zoom of the SNR close to the time of the merger in the case of black holes with the same masses.

Figure 4.3: SNR with the detectable duration of time in second(s). The two figure is detected from LIGO Hanford (pink) and LIGO Livingston(green). The two-wave signals are the same but the amplitude of the wave detected at Hanford detector is longer than the wave detected from Livingston detector and these are similar to the gravitational wave predicted from the merger of the binary black hole or binary neutron stars.

in Livingston detector. For both sets of parameters, we see that the two LIGO detectors present a clear peak above the noise.

4.1.4 Change of the waveform with the mass of the binary

We can also see how the parameters change the dimensions of the gravitational wave signal. The magnitude of the gravitational waves depends on the separation from the source and therefore the second derivative of the mass dispersion (mass times acceleration within the case of one particle). Hence, one must consider exceptionally enormous objects moving brutally as the candidates for the sources of detectable gravitational waves. The foremost promising candidates are compact binaries consisting of either two neutron stars, two black holes or one neutron star, and one black hole. They are small and heavy, which allows them to orbit at a closer distance and at a high orbital frequency, which suggests that the second derivative of the mass distribution of the system is large. Therefore, the system emits strong gravitational waves.

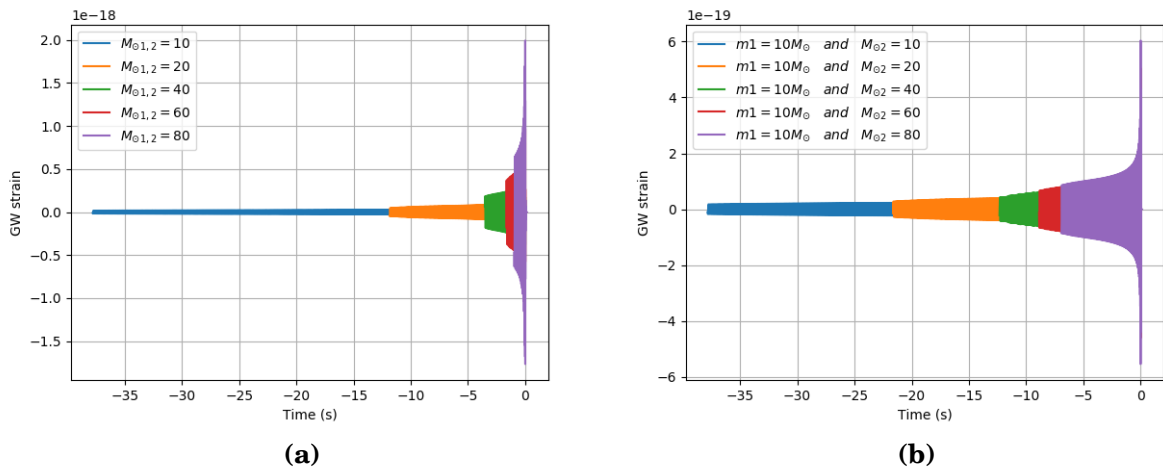


Figure 4.4: Gravitational wave signal for different mass of binary system for the IMRPhenomB model. We see that the amplitude, as well as the frequency are modified, from the in-spiral to the ring-down phase. The left panel constructed from two equal masses of black holes the amplitude of wave is small compared to the right one. The right panel one mass of the black hole kept fixed ($10 M_{\odot}$) whereas the second masses free to change.

We know mass is a source of gravity, so events that have greater mass it also have strong gravity. As shown in Fig.4.4 as the mass of the binary increases the amplitude of the gravitational wave signal increases and the black hole becomes more denser.

4.1.5 Change of the waveform with distance from the source of the binary

The magnitude of the gravitational waves depends on the separation from the source. The maximum amplitude of the relative change in length was about 10^{-23} . These exact analyses of the signal based on the theory of general relativity should that it come from merging black holes with $25 M_{\odot}$ at lower frequency of 30 Hz(left panel) and $15 M_{\odot}$ at lower frequency of 25 Hz(right panel) of Fig.4.5 which is merged at a distance of 100 Mpc, 200 Mpc, 300 Mpc and 500 Mpc from the Earth. The dimensionless gravitational-wave amplitude $h = \Delta L/L$ (the "strain") is proportional to the amount of out-going laser light. The fact that the directly-measurable quantity is the amplitude $h \propto \frac{1}{r}$, not the energy of the wave as in the electromagnetic antenna.

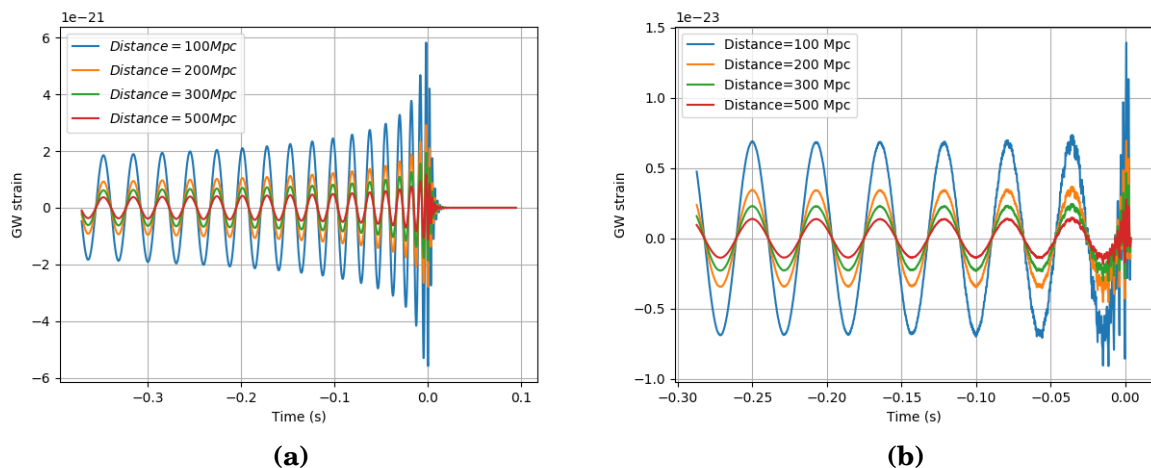


Figure 4.5: Gravitational wave amplitude detecting at different distance from the Earth and variation of waveform models SEOBNRv4(left panel) and IMRPhenomA(right panel).

From Fig.4.5 we can see the amplitude of the gravitational wave depends on the distance from the source. The gravitational wave from binary black holes or binary neutron star mergers is like standard siren's their amplitude falls off like $\frac{1}{r}$. So their amplitude at the detector on Earth tells us how far away they are. The

variation of gravitational wave amplitude with inverse law gives us a lot of hope for detecting ultra-distance gravitational wave that brings information from very far distant galaxies.

4.1.6 Waveform comparison

Fig.4.6 shows the gravitational waveform obtained by SEOB, phenomenological model and the LIGO detection those have the same wave properties. When the black holes come sufficiently close, the velocities are relativistic and gravity is strong, Inevitably, black holes dive towards each other and collide at the velocity close to the speed of light; the black holes merge together to make a single remnant black hole. In Fig.4.6 the data from each of the detectors can be lined up against

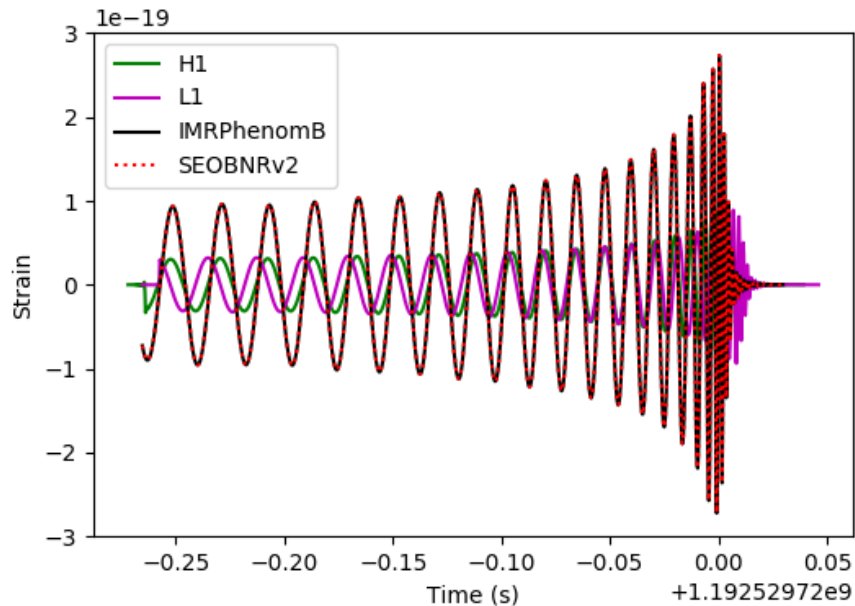


Figure 4.6: Time domain waveform SEOBNR stands for Spin Effective One Body Numerical Relativity, this model is calibrated to a set of numerical relativity simulations and frequency domain IMRPhenom, stands for phenomenological In-spiral-Merger-Ring down model, the models of the waveform by phenomenological predicting the amplitude and phase evolution. This waveform family is also calibrated to a set of numerical relativity simulations.

each other. We also check that the data from the detectors are consistent with each other, both detectors see similar astrophysical signals and it also have similar characteristics to the time domain waveform modeled by SEOBNRv2(red dotted) and IMRPhenomB-(black). If GR agrees with the observed signals, both estimates of the final BH's mass and spin should agree with each other. For gravitational

waves emanating from the inward spiral and merge of pair of black holes, the waveform detected in LIGOs and the two wave models "IMRPhenom" and "SEOBNR" are aligned with each other.

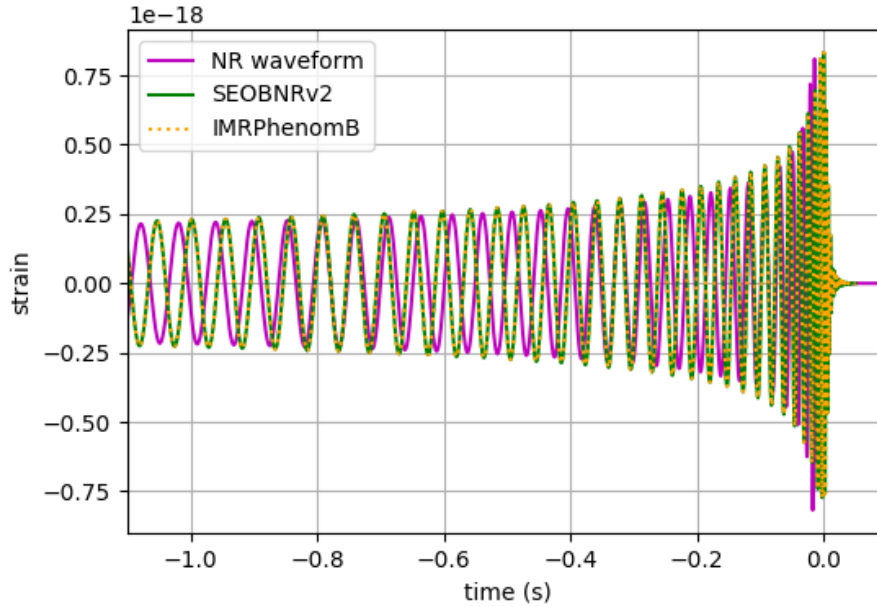


Figure 4.7: waveform comparison between NR, SEOBNRv2 and IMRPhenomB wave models.

Fig.4.7 is formed from binary black hole mass of $m_1 = 41 M_\odot$ and $m_2 = 29 M_\odot$ with lower frequency of 10Hz. As we have seen earlier when the binary black hole close to each other specially around the merger, Einstein general relativity prediction is solved by numerical relativity. The solition of general relativity simulated by numerical relativity and our gravitational models from SEOBNR and IMRPhenom around the merger are matched with each other, so from this verification we can understand that GR passes the test of gravitational wave.

4.2 Summary

In this chapter we summarize the results obtained from the modern falsfication test of general relativity with gravitational wave using the data from the GW150914 NR waveform and we have comper the result to the phenomological and SEOBNR waveforms. The result helps to produce a good match between general relativity and gravitational wave, therefore the detection of gravitational wave from the binary source asserts that gravitational wave verify Einstein general theory of relativity.

Conclusion

In Einstein general theory of relativity, gravity is treated as phenomenon resulting from the curvatur of space time. These propageting phenomena are gravitational waves, as gravitational wave passess an observer, that obsever will find space time distorted by the effect of strain, that is gravitational wave could be the natural out come of general theory of relativity, which says that very massive objects distort the fabric of time and space. GW are pridiction of GR-theory of space and time (space-time), and mater and energy. It gives us the oppportunity to test GR in the strong field, highly dynamical regim. Most tests of GR have taken place under the relatively weak-gravity conditions of the solar system or of binary pulsars. Linear approximation of Einstein field equations, numerical relativity wave form, effective one body wave model, the IMR phenomenological wave model and detection of GW by LIGO are consistent with pridiction of GR in the highly dynamical(strong field) regim. All these result leads us to generalized the Einstein general theory of relativity passess the test of GW. Threfore, gravitational wave measurements will allow us to directly probe some of the most violent events in the universe, to directly measure the most tumultuous dynamics of spacetime geometry. Gravitational waves would allow us to probe how space time really behaves under the most radical of circumstances and teles us the univers is expanding. It is also important to detect gravitational waves because they would bring new information from distant galaxies in which electromagnetic waves cannot, it could also directly prove GR. Although, as we have just said, we consider that the goal of the thesis has been accomplished, there are plenty of improvements that could be done in order to achieve better results. This opens the oppportunity to extend the study of Einstein general theory of relativity in cosmology as future work.

Bibliography

- [1] Yunes, Nicolás and Siemens, Xavier. Gravitational-wave tests of general relativity with ground-based detectors and pulsar-timing arrays, *Living Reviews in Relativity*, 16(1):9, 2013.
- [2] Riles, Keith. Gravitational waves: Sources, detectors and searches, *Progress in Particle and Nuclear Physics*, 68:1–54, 2013.
- [3] Lommen, Andrea N. Pulsar timing arrays: the promise of gravitational wave detection, *Reports on Progress in Physics*, 78(12):124901, 2015.
- [4] LIGO Scientific Collaboration and others. Gravitational wave astronomy with LIGO and similar detectors in the next decade, *arXiv preprint arXiv:1904.03187*, 2019.
- [5] Brüggmann, Bernd. Fundamentals of numerical relativity for gravitational wave sources, *Science*, 361(6400):366–371, 2018.
- [6] Usman, Samantha A and Nitz, Alexander H and Harry, Ian W and Biwer, Christopher M and Brown, Duncan A and Cabero, Miriam and Capano, Collin D and Dal Canton, Tito and Dent, Thomas and Fairhurst, Stephen and others. The PyCBC search for gravitational waves from compact binary coalescence, *Classical and Quantum Gravity*, 33(21), 2016.
- [7] Bender, PL and Brillet, A and Ciufolini, I and Cruise, AM and Cutler, C and Danzmann, Karsten and Folkner, WM and Hough, J and McNamara, PW and Peterseim, M and others. LISA. Laser Interferometer Space Antenna for the detection and observation of gravitational waves. An international project in the field of Fundamental Physics in Space, 1998.
- [8] Ryder, Lewis Introduction to general relativity, Cambridge University Press publisher, 2009.

- [9] Claus Lammerzahl(claus.laemmerzahl@zarm.uni-bremen.de) Volker Perlick (volker.perlick@zarm.uni-bremen.de), Gravitational Waves-ZARM-Uni Bremen.
- [10] Patrick J. Sutton. Introduction to General Relativity and Gravitational Waves, International School of Physics "Enrico Fermi" Varenna, 2017/07/03-04
- [11] Degollado, Juan Carlos. The detection of gravitational waves, *Journal of Physics: Conference Series*, 912(1):012018, 2017.
- [12] Huwyler, Cédric. Testing General Relativity with Gravitational Waves, 2014.
- [13] Królak, Andrzej and Patil, Mandar. The first detection of gravitational waves, *Universe*, 3(3):59, 2017.
- [14] Varma, Vadapalli Vijay S. Black hole simulations: from supercomputers to your laptop, 2019.
- [15] Gareth P. Alexander. PX436: General Relativity, University of Warwick email: G.P.Alexander@warwick.ac.uk: 2017.
- [16] Li, Tjonnje GF Extracting physics from gravitational waves: testing the strong-field dynamics of general relativity and inferring the large-scale structure of the Universe, 2015.
- [17] Marie Anne Bizouard, LAL Gravitational wave transient sources, PNHE TS2020 2nd workshop June 4th 2018, Montpellier.
- [18] Da Silva Costa, Carlos Data analysis pipeline for the spherical gravitational wave antenna MiniGRAIL, 2010.
- [19] Bello Arufe, Aaron. Gravitational Waves in General Relativity, 2017.
- [20] Fields, CE and Li, TGF and Isi, M and Weinstein, A Testing The Strong Field Dynamics of General Relativity Using Compact Binary Systems.
- [21] Sathyaprakash, Bangalore Suryanarayana and Schutz, Bernard F Physics, astrophysics and cosmology with gravitational waves, *Living reviews in relativity*, 12(1):1-141, 2009.
- [22] Cervantes-Cota, Jorge L and Galindo-Uribarri, Salvador and Smoot, George F. A brief history of gravitational waves, *Universe*, 2(3):22, 2016.
- [23] Baumgarte, Thomas W and Shapiro, Stuart L. *Binary black hole mergers Physics Today*, 64(10):32, 2011.

- [24] Marchand, Tanguy. Studying gravitational waves of compact binary systems using post-Newtonian theory, 2018.
- [25] Will, Clifford M. Was Einstein right? A centenary assessment, *arXiv preprint arXiv:1409.7871*, 2014.
- [26] Sampson, Laura Mae and others. Testing general relativity with gravitational waves, 2014.
- [27] Ghosh, Abhirup and Johnson-McDaniel, Nathan K and Ghosh, Archisman and Mishra, Chandra Kant and Ajith, Parameswaran and Del Pozzo, Walter and Berry, Christopher PL and Nielsen, Alex B and London, Lionel. Testing general relativity using gravitational wave signals from the inspiral, merger and ringdown of binary black holes, *Classical and Quantum Gravity*, 35(1):014002, 2017.
- [28] Abbott, Benjamin P and Abbott, R and Abbott, TD and Abernathy, MR and Acernese, F and Ackley, K and Adams, C and Adams, T and Addesso, P and Adhikari, RX and others. Tests of general relativity with GW150914, *arXiv preprint arXiv:1602.03841*, 2016.
- [29] Kokkotas, Kostas D. Gravitational wave physics, *Encyclopedia of Physical Science and Technology*, 7(3):67–85, 2002.
- [30] Marx, Jay and Danzmann, Karsten and Hough, James and Kuroda, Kazuaki and McClelland, David and Mours, Benoit and Phinney, Sterl and Rowan, Sheila and Sathyaprakash, B and Vetrano, Flavio and others The Gravitational Wave International Committee Roadmap: The future of gravitational wave astronomy, *arXiv preprint arXiv:1111.5825*, 2011.
- [31] Hobson, Michael Paul and Efstathiou, George P and Lasenby, Anthony N, General relativity: an introduction for physicists, 2006.
- [32] Nasir, Fahad. Simulation of gravitational waves and binary black holes spacetimes, 2010.
- [33] Mastandrea, Radha and Mentor, MIT and Weinstein, Alan. Testing General Relativity with Binary Black Hole Mergers.
- [34] Pürrer, Michael and Hannam, Mark and Ajith, P and Husa, Sascha. Testing the validity of the single-spin approximation in inspiral-merger-ringdown waveforms, *Physical Review D*, 88(6), 2013.

- [35] Bhagwat, Swetha. Towards Probing The Strong Field Gravity Using Binary Black-Hole Ringdowns, 2019.

DECLARATION

ADDIS ABABA UNIVERSITY
COLLEGE OF NATURAL AND COMPUTATIONAL SCIENCES
DEPARTMENT OF PHYSICS

MSc Thesis

Verification of Einstein General Theory of Relativity with Gravitational Waves

Name of Candidate: Abel Habtie Alemu

I the under signed declare that the thesis is my original work and no part of it can be claimed as an intellectual property of anybody else except me and my advisors.

Signature: _____